Acurex Technical Report TR-82-02/AD

DEVELOPMENT OF A ROTARY INSTRUMENTATION SYSTEM PHASE II

by Alan Adler and William Skidmore

ACUREX CORPORATION

prepared for

NATIONAL AERONAUTICS AND SPACE ADMINISTRATION

NASA Lewis Research Center
Contract NAS 3-20796

1. Report No.	2. Government Accession No.	3. Recipient's Catalog No.

4. Title and Subtitle	5. Report Date
Development of a Rotary Instrumentation System -- Phase II	December 1982
	6. Performing Organization Code

7. Author(s)	8. Performing Organization Report No.
A. Adler and W. Skidmore	
	10. Work Unit No.

9. Performing Organization Name and Address	11. Contract or Grant No.
Acurex Corporation Mountain View, California	NAS 3-20796
	13. Type of Report and Period Covered
12. Sponsoring Agency Name and Address	Contract Report
National Aeronautics and Space Administration	14. Sponsoring Agency Code

15. Supplementary Notes

16. Abstract

ABSTRACT

This Phase II report describes continued development of an advanced telemetry instrumentation system for measuring strain and temperature on the rotating components of high-speed turbomachinery. The system differs from existing systems in that the rotating transmitters encode the measurement data onto the carriers which are phase-locked to a reference frequency. The rotating electronics are powered by a 200 kHz rotary induction system which also provides the reference frequency for the phase-locked transmitters. Initial design and systems analysis was described in the Phase I report, NASA CR-159453. This report describes the results of continued development and the fabrication and environmental testing of a small system.

17. Key Words (Suggested by Author(s))	18. Distribution Statement
	Unclassified - unlimited

19. Security Classif. (of this report)	20. Security Classif. (of this page)	21. No. of Pages	22. Price*
Unclassified	Unclassified	86	

*For sale by the National Technical Information Service, Springfield, Virginia 22151

TABLE OF CONTENTS

TABLE OF CONTENTS (Concluded)

LIST OF FIGURES

LIST OF TABLES

SUMMARY

This Phase II report describes continued development of an advanced telemetry instrumentation system for measuring strain and temperature on the rotating components of high speed turbomachinery. Initial design and systems analysis was described in the Phase I report, NASA CR-159453. For clarity, a summary of the work performed under Phase I is listed below:

- Systems analysis of the "communications link" (channel carrier spacing, crosstalk, signal-to-noise ratio, etc.)
- Design and testing of typical antenna systems
- Circuit design and breadboard testing of:
  - -- Two alternate receivers
  - -- Three alternate static strain modulators
  - -- A phase-locked FM transmitter
- Transmitter package design including development of fabrication techniques and component selection for operation at up to 175°C and 50,000 g's centrifugal force
- Fabrication of prototype transmitter and testing at 175°C combined with 40,000 g's

The work performed under Phase II is a continuation of the Phase I effort. This work is listed below:

1. Further circuit design, printed circuit layout, and packaging of the stationary electronics
2. Assembly and testing of the stationary electronics
3. Design and development of a custom integrated circuit which is the phase-locked frequency synthesizer in the rotating transmitter module
4. Breadboard testing of a static strain transmitter module
5. Design and development of a new, lightweight, carbon fiber transmitter packaging system
6. Fabrication and environmental testing of a small number of channels of the stationary and rotating electronics
7. System testing and demonstration of the potential to expand the system to a large number of channels
8. Delivery of a small system to NASA-Lewis Research Center

SECTION 1

INTRODUCTION

This report describes the Phase II activities of NASA Contract NAS3-20796 for the design and development of a rotary instrumentation system.

A rotary instrumentation system consists of ruggedized miniature telemetry transmitters installed on the rotating shaft of a gas-turbine engine to telemeter the outputs of sensors (strain gages, thermocouples, etc.) on rotating engine components.

The development program commenced in mid-1976 with Phase I, which was system design and research into high temperature and high G packaging. The results of Phase I are documented in reference 1.

Phase II called for the development of a small prototype system, to demonstrate the capabilities of performing in the intended environment and also to demonstrate that the system was expandable to handle about 100 data channels.

Phase II met the system design objectives, however, scope was reduced in mid-program to conserve funds. This was necessary because of difficulties incurred by a major subcontractor (RCA Semiconductor Division) in supplying a key custom integrated circuit. The subcontractor was more than three years late in delivering this circuit. This, of course, also greatly delayed completion of this phase of the program.

Although the late delivery of the integrated circuit caused unanticipated expenses which resulted in the reduction of scope, one benefit resulted from the delay. Continued development in packaging of the engine-mounted transmitters resulted in a design breakthrough which reduced the weight of each transmitter an order of magnitude (from 30 grams to 4 grams) and also reduced manufacturing costs. The new packaging method is detailed in the body of this report.

1.1 SYSTEM CONCEPT

As with previous rotating instrument systems, this system consists of two subsystems (see figure 1-1):

a. Rotating Subsystem

   Shaft-mounted electronics which interface with the transducers (strain gages, thermocouples or pressure transducers) and encode their signals onto carriers and/or subcarriers for transmission to a stationary subsystem.

b. Stationary Subsystem

   Receivers and demodulators which decode the signals from the rotating system and restore them to amplified analogs of the original transducer outputs.

This stationary system also includes a 200 kHz power supply which couples power inductively (without physical contact) to the electronics of the rotating system.

The most important difference between this new system and previous systems is that the inductively coupled power is also employed as a reference clock to synchronize the carrier frequency of each transmitter. Furthermore, this same 200 kHz signal is employed as a reference to the receivers of the stationary system.

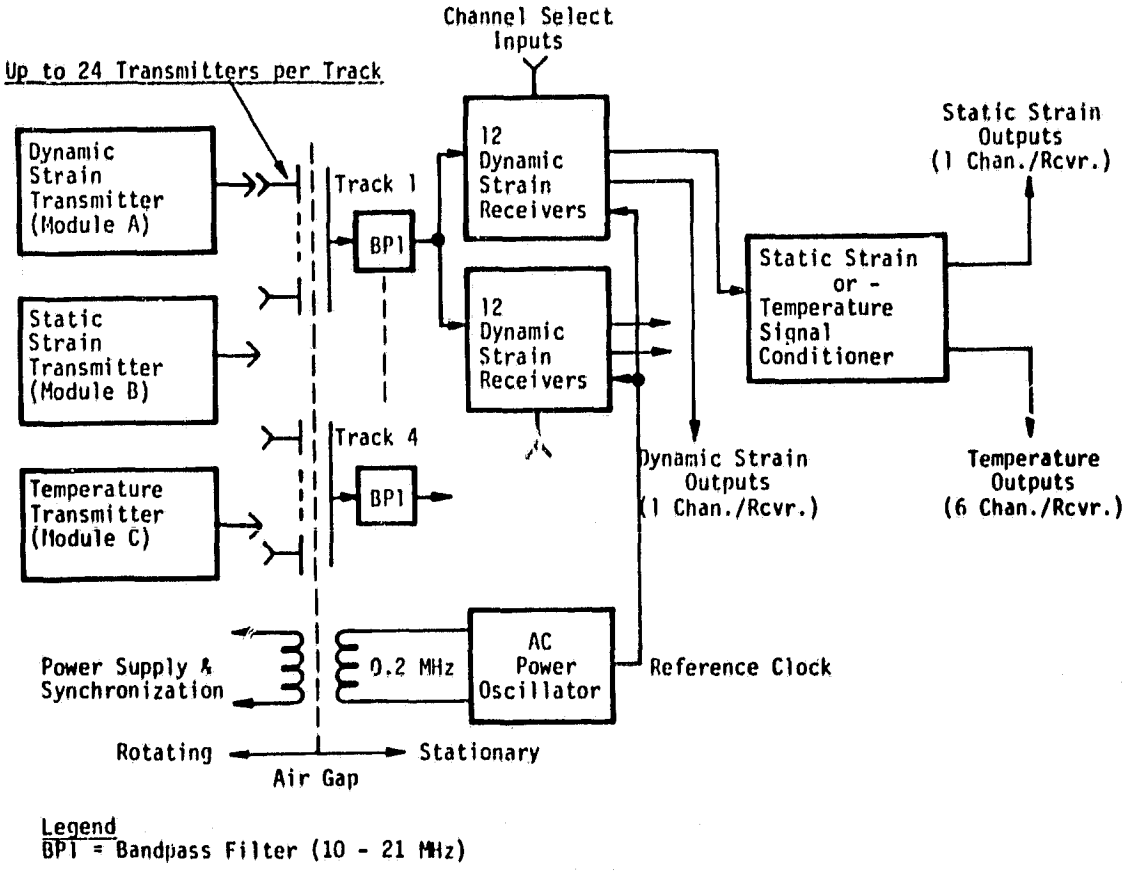

Figure 1-1. System Block Diagram

This permits precise digital tuning by merely selecting the desired channel number on the receiver.

1.1.1 Rotating Electronics

The system includes three basic types of transmitter modules:

- Module A -- Dynamic strain transmitter
- Module B -- Static strain transmitter
- Module C -- Temperature transmitter containing six time-division multiplexed thermocouple channels

The physical locations of the modules in relation to the engine shaft and the capacitive antenna tracks is shown in figure 1-2. In this example there are four layers of modules. Each layer consists of up to 24 RF channels and is sensed a small distance away by a narrow conducting circular strip which acts as an antenna track. The four tracks are mounted on a stationary insulated disc with a grounded plane on its opposite side. In addition, grounded guard bands are placed between the tracks in order to reduce crosstalk. Further reduction of crosstalk between adjacent tracks is achieved by alternating the tracks with odd- and even-numbered channels. The channel frequency allocations are shown in Table 1-1.

Each channel carrier is frequency modulated with a nominal frequency deviation of ±75 kHz. The modulating frequency band ranges from 20 Hz to 40 kHz.

1.1.2 Stationary Electronics

The stationary electronics consists of the following equipment:

- Induction power oscillator
- Receiver system
  - -- System clock
  - -- Receiver cards (output is analog of dynamic strain signal

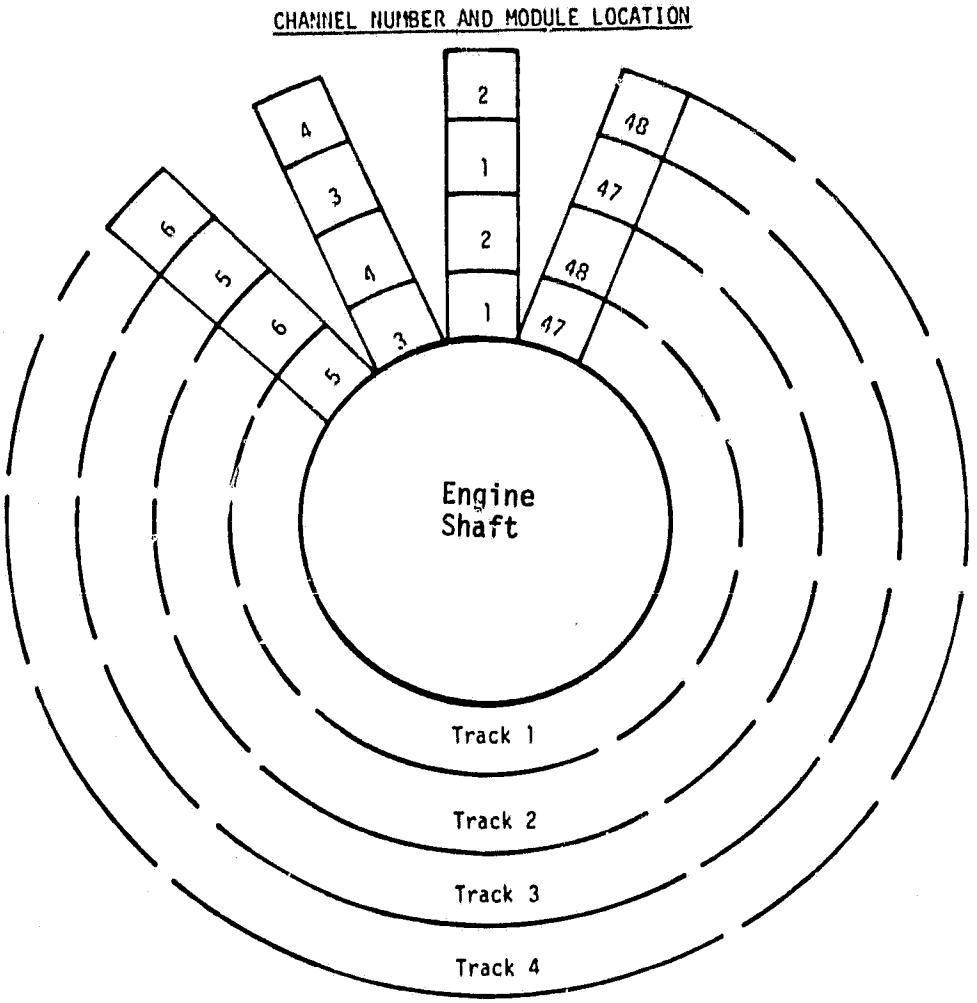

Figure 1-2. Module locations

Table 1-1. Channel Frequency Allocations

Channel No.	Frequency	Channel No.	Frequency
1	11.493 MHz	30	17.239 MHz
2	11.691	31	17.437
3	11.889	32	17.635
4	12.087	33	18.833
5	12.285	34	18.031
6	12.483	35	18.230
7	12.681	36	18.428
8	12.880	37	18.626
9	13.078	38	18.824
10	13.276	39	19.022
11	13.474	40	19.220
12	13.672	41	19.419
13	13.870	42	19.617
14	14.069	43	19.815
15	14.267	44	20.013
16	14.465	45	20.211
17	14.663	46	20.409
18	14.861	47	20.607
19	15.059	48	20.806
20	15.257	49	21.004
21	15.456	50	21.202
22	15.654	51	21.400
23	15.852	52	21.598
24	16.050	53	21.796
25	16.248	54	21.994
26	16.446	55	22.193
27	16.644	56	22.391
28	16.843	57	22.589
29	17.041	58	22.787

-- Static strain or temperature demodulator cards (when required)

The induction power system is described in paragraph 3.3

1.1.3 Receiver System

Referring to figure 1-1, note that each group of up to 24 dynamic strain receivers is preceded by a bandpass filter (BP1). Bandwidth and group delay characteristics should be such that the fundamental frequency components of all incoming frequency-modulated carriers are passed virtually distortion free.

Its purpose is twofold:

- Prevention of receiver input saturation due to crosstalk from the inductive power system
- Reduction of the receiver image frequency response due to transmitter carrier harmonics

Each receiver frequency is digitally programmable. Any of its outputs may be selected for either dynamic strain, static strain or temperature measurements.

For dynamic strain, which employs direct frequency modulation, the outputs of the receivers are ready-to-use analogs of the original strain gage signals.

For static strain or temperature the D.C. data is encoded onto a 3 kHz subcarrier and additional signal processing is performed by static strain or temperature demodulating cards which restore the signals to analogs of the original sensor signals. These demodulator cards are plugged-in (when required) to the receiver. The receiver chassis is 19 inches wide, rack-mountable, and accepts up to 12 plug-in cards which may be receivers, demodulators or mixes of each.

SECTION 2

ROTATING ELECTRONICS

This section covers the following topics:

- Dynamic Strain Transmitter
- Antenna System
- Induced Power System
- Packaging Techniques
- Design Goals

2.1 DYNAMIC STRAIN TRANSMITTER

Figure 2-1 is a block diagram of this module. This module contains the following subsystems:

- An isolated, regulated DC power supply which receives 200 kHz AC power from the induced power system (see section 2.3) and produces a regulated 8 VDC to power the circuitry within the module. Isolation is provided by an individual power transformer within the module. The isolation permits accurate strain measurements with grounded gages.
- A 10 mA constant-current regulator which supplies excitation to the strain gage. Constant-current regulation was not originally planned but was incorporated into the design during this development phase in response to industry requests. They prefer

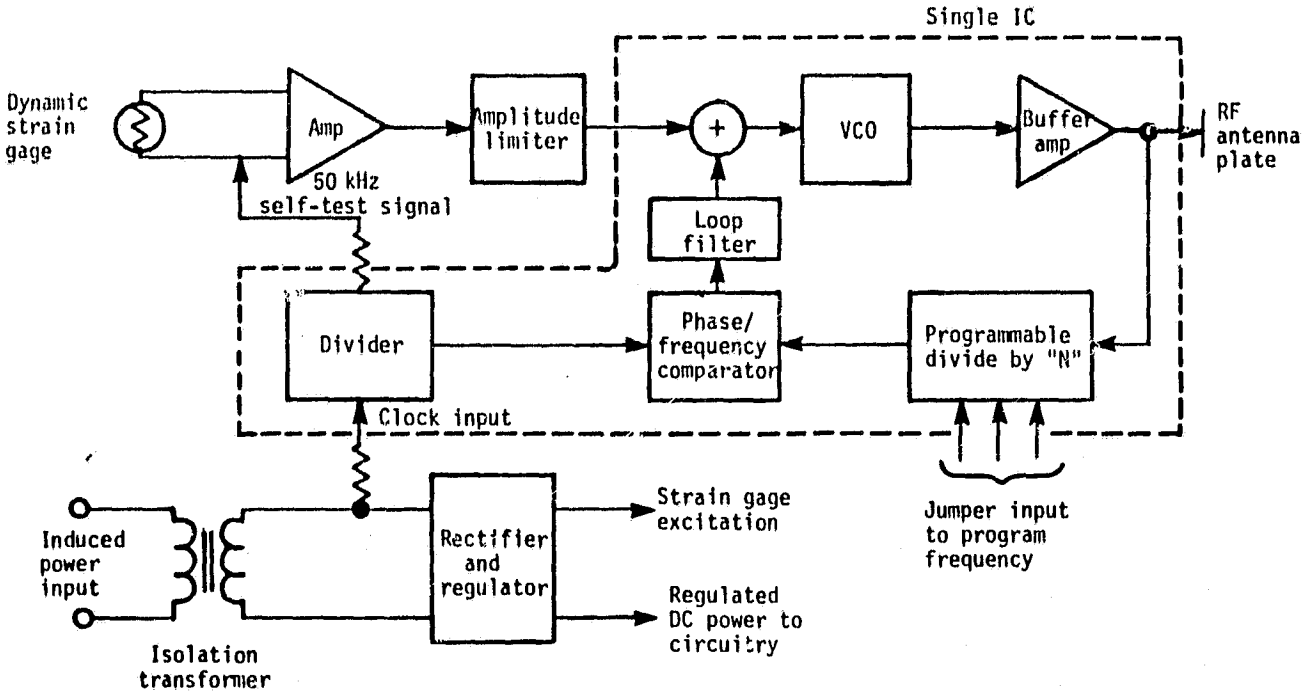

Figure 2-1. Dynamic Strain Transmitter (Block Diagram)

constant-current excitation because it eliminates variations in strain signal due to variations in lead wire resistance.

- An AC amplifier for amplifying the dynamic strain signals from the gage
- A 50 kHz self-test circuit. A 50 kHz signal, derived by dividing the induced power signal by 4, is injected into the input of the AC strain amplifier. If the strain gage circuit becomes open (due to an open gage or an open lead wire) the accompanying change in DC voltage at the constant-current output will bias a transistor (which supplies bias current to the amplifier) to its off state. When this occurs the amplifier can no longer amplify the 50 kHz self-test signal and it disappears from the transmitted RF carrier signal. The absence of the 50 kHz is detected in the stationary receiver and a visual and electronic indication is activated.
- A synchronized FM transmitter which is phase-locked to the 200 kHz induced power voltage by a custom designed frequency synthesizer IC. It is the IC which was several years late and caused the severe program delays.

2.1.1 Static Strain Transmitter -- Breadboard Development

A block diagram of the static strain transmitter is shown in figure 2-2. Note that the output of the strain gage bridge is modulated by a chopper which is being driven at 3.1 kHz by a signal derived by dividing the 200 kHz square wave. This chopper output, which is equal in amplitude to the instantaneous DC output of the strain gage bridge, is amplified and telemetered by a system identical to that employed for the telemetry of dynamic strain (except that the 50 kHz test signal of dynamic strain is deleted).

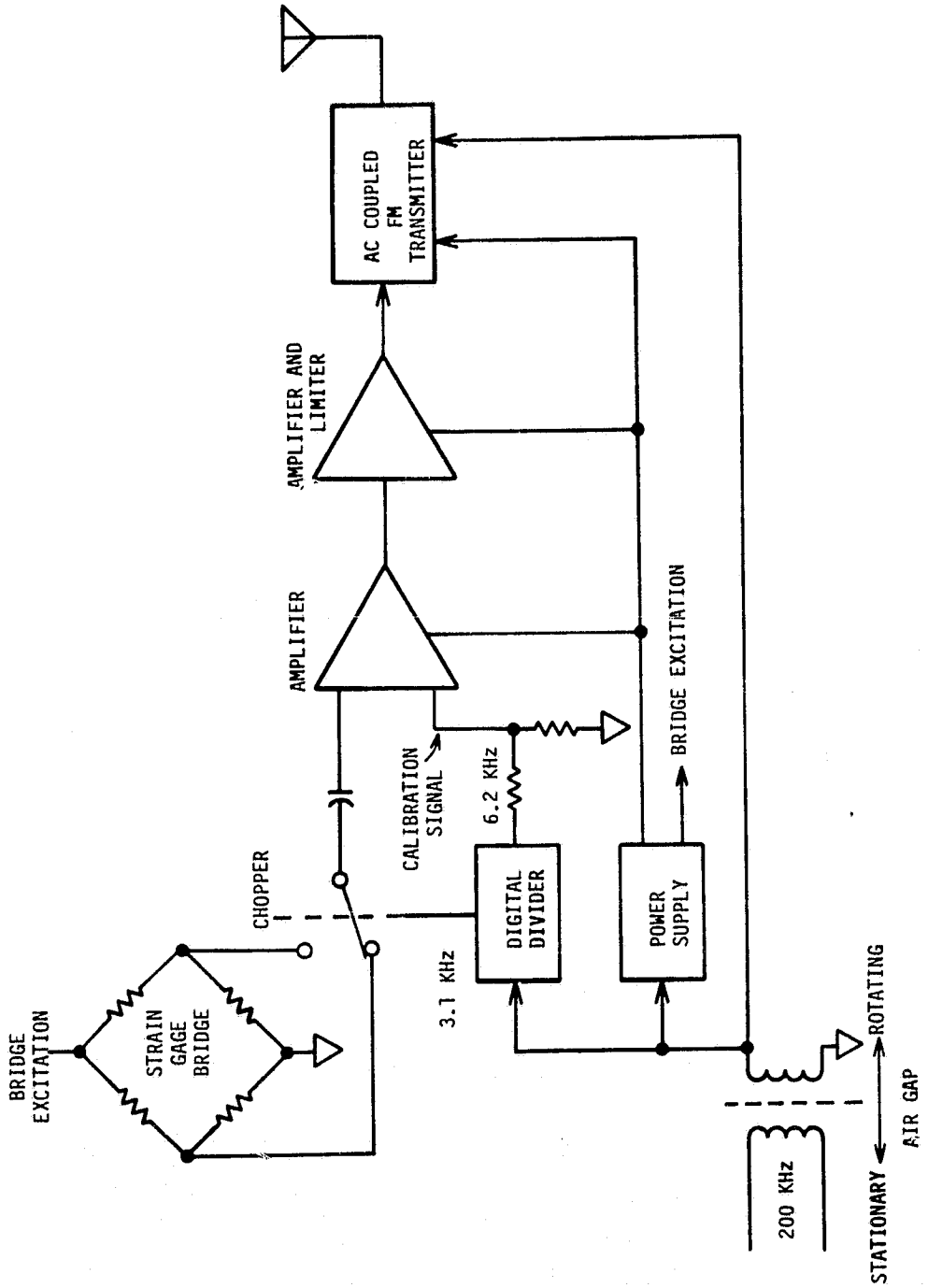

Figure 2-2. Block Diagram of Static Strain Transmitter

In addition to the elements described above, note that a 6.2 kHz calibration signal, also derived by dividing the 200 kHz induction frequency, is injected directly into the input of the AC strain amplifier. The amplitude of the calibration signal is determined by the voltage of the module's internal DC voltage regulator and can be made stable, or set to any desired positive or negative temperature coefficient. The transmitter telemeters a composite signal, which is the sum of the 3.1 kHz strain signal and the 6.2 kHz calibration signal.

In the receiver, the amplitude of the 6.2 kHz calibration signal is demodulated and compared to a reference to control an AGC loop. The loop varies the amplitude of the entire composite signal in order to maintain the 6.2 kHz component constant. This allows automatic self-calibration of variations in the gain of the telemetry channel. A more detailed description of the self-calibration system can be found beginning on page 148 of the Phase I report (reference 1).

The method of static strain modulation and telemetry is attractive because of its simplicity and its utilization of nearly all of the circuitry of the dynamic strain transmitter. It is even possible for the same microcircuit substrate to be employed for both static and dynamic strain transmitters -- with slight changes in die attachment and wire bonding to determine the transmitter type. This method of telemetering static strain was developed and patented (reference 4) many years ago at Acurex and is the basis of their model number 206 transmitter.

In addition to its simplicity and its utilization of the dynamic strain circuitry, the modulation method offers excellent zero stability. The zero stability is determined primarily by the leakage current of the field-effect transistors employed in the chopper. In practice, zero drifts of only a few

microvolts can be achieved over a range of ambient temperature variations of more than 100°C.

The gain stability of the system (without self-calibration) is largely determined by the gain stability of the AC amplifier and VCO -- which are the "dynamic strain" part of the system. In practice it is the gain stability of the VCO which requires the most attention to compensate against temperature variations.

Referring to Table 2-1 of this report, note that the allowable errors for the static strain system were given as about half of those allowed for the dynamic strain system. This was in response to the user data provided to the AFAPL Study of Industry Requirements (reference 2). The self-calibration system described above was designed in order to meet the tighter accuracy requirements of static strain.

A schematic diagram of the breadboard static strain modulator is shown in figure 2-3 which shows the implementation of the block diagram in figure 2-2.

The breadboard was tested for zero stability, linearity, and gain stability versus temperature. Initial results showed a gain stability which was inferior to that of the system without self-calibration. A series of tests were initiated to isolate the cause of the problem -- which was believed to be intermodulation between the 3.1 kHz strain signal and the 6.2 kHz self-calibration signal. Unfortunately reduction of project scope, necessitated by the delays in delivery of the frequency synthesizer IC, terminated these tests before their completion. However, it is believed that the basic system of self-calibration is valid -- judging from analysis and from the good results obtained with self-calibration in the thermocouple telemetry system already in production (reference 5).

Table 2-1. Table of Performance Goals

Charcteristic	Limit	Strain or Pressure		Temperature
		Dynamic	Static	
Accuracy	Minimum	±5%	±2%	±0.5%
	Design goal	±2%	±1%	
Frequency range	---	10 Hz to 30 kHz	0 to 500 Hz	0 to 25 Hz
Most sensitive full-scale range	---	500μ strain	500μ strain	29 mV
Phase correlation (Channel-to-channel)	Minimum	±10° (to 30 kHz)	±10° (to 500 Hz)	---
	Design goal	±5° (to 30 kHz)	±10° (50 500 Hz)	
Ambient temperature range	Minimum	0°C to 150°C		
	Design goal	0°C to 175°C		
Centrifugal force limit	Minimum	40,000 g's		
	Design goal	50,000 g's		

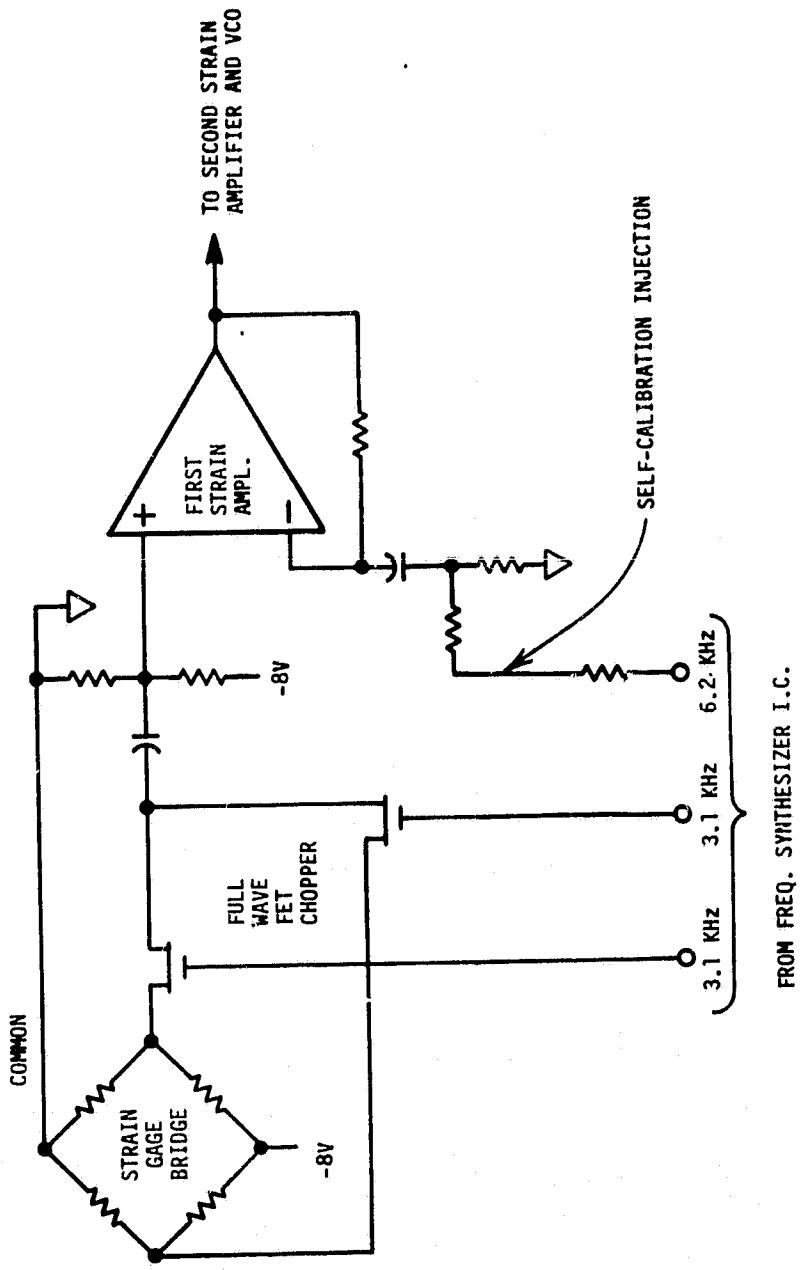

Figure 2-3. Schematic Diagram Static Strain Modulator

2.2 ANTENNA SYSTEM

Each rotating transmitter has a small antenna plate mounted at its end. The frequency modulated RF outputs of the transmitters are capacitively coupled through these plates to a stationary antenna. Figure 2-4 illustrates the preferred arrangement. The system is intended to function with spacing in the range of 0.02 to 0.15 in.

The stationary antenna is comprised of a series of concentric, co-planar conductive rings which are fabricated on a disc of glass-epoxy or glass-polyimide printed circuit stock. The rings may be cut on a lathe or by conventional printed circuit etching techniques.

Note in figure 2-4 that there is a grounded guard-ring between each of the active antenna rings. This is to enhance electrical isolation between the antenna rings. To provide a good RF ground, the back plane of the antenna disc is conductive. The antenna used for the tests is illustrated in figure 2-5.

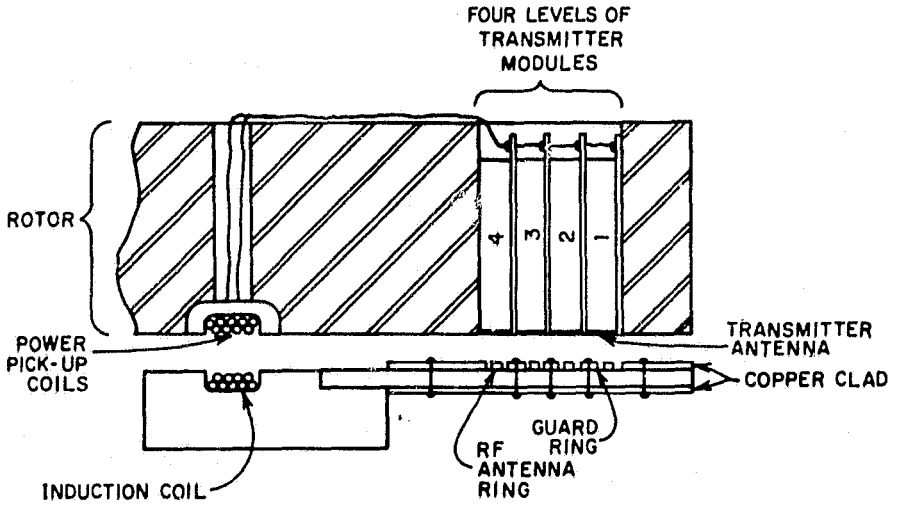

Figure 2-4. Side View of Transmitters, Antenna, and Ground Plane

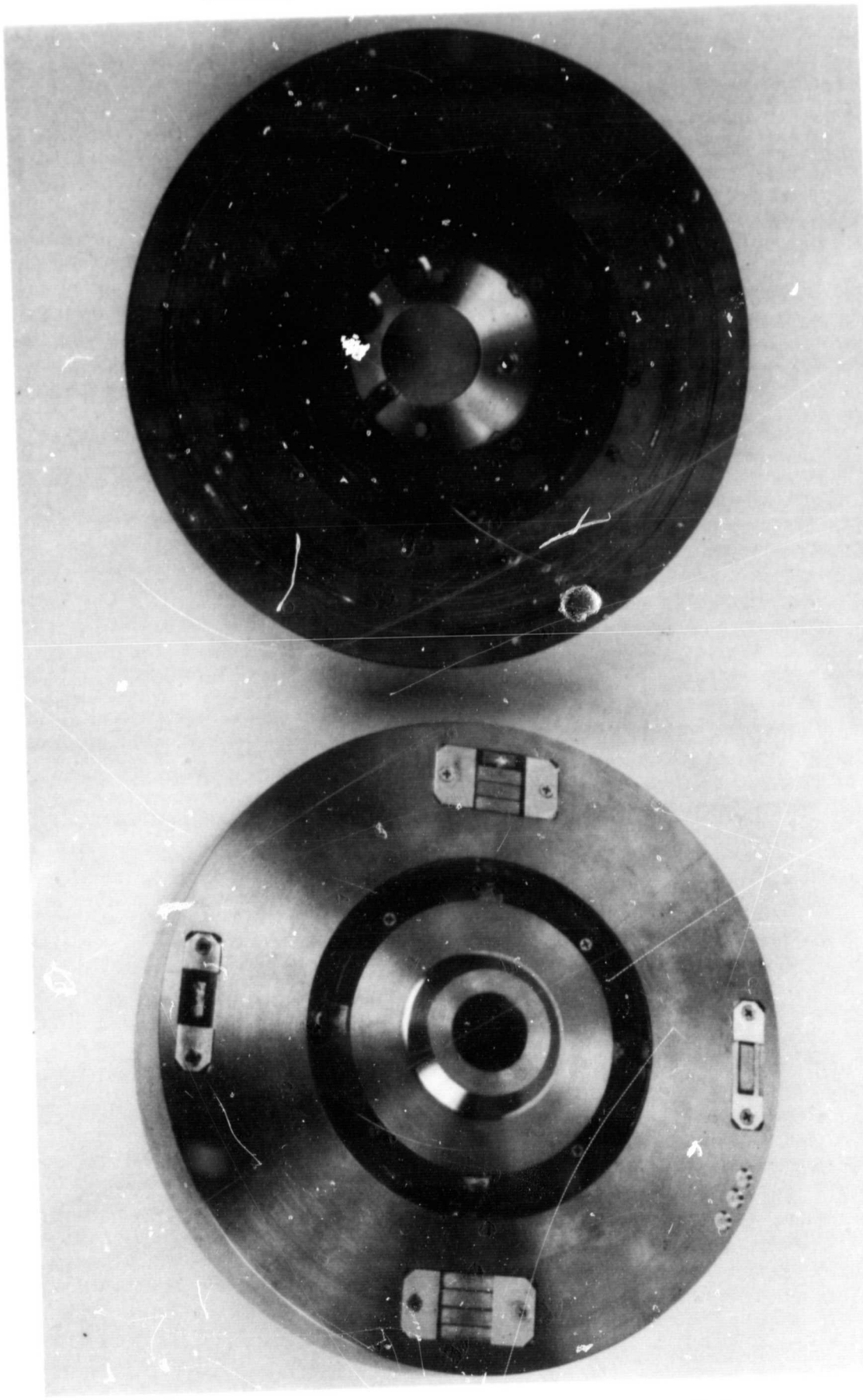

Figure 2-5. Stationary and Rotating Antenna Halves

2.3 INDUCED POWER SYSTEM

The induced power system couples 200 kHz power from a stationary induction oscillator to the rotating transmitters via an air core rotary transformer with a rotating secondary winding. Each transmitter has a built-in isolation transformer, which also serves to step up the voltage from the secondary winding. A single secondary winding can serve a number of rotating transmitters.

The primary and secondary windings are wound from magnet wire (coated with high temperature insulation) and impregnated with epoxy. The exact number of turns employed on each winding is not critical, but is usually calculated to yield an inductance in the range of approximately 100 microhenries. The winding is resonated at 200 kHz (with a variable capacitor in the induction oscillator) to maximize power transfer and aid in suppressing harmonics.

Figures 2-4 and 2-5 also illustrate the induced power coils. Figure 2-6 illustrates the induction oscillator.

2.4 PACKAGING TECHNIQUES

As mentioned in the introduction, the long delays in delivery of the custom frequency synthesizer IC provided time for a significant advance in packaging.

Previous transmitters have been fabricated with hybrid microcircuitry on ceramic substrates. These substrates are relatively brittle and inflexible and require rigid metal enclosures to protect them. The metal enclosures comprise most of the weight and a significant portion of the manufacturing cost of the finished transmitter.

An additional problem with the metal enclosures is that they normally are made from low-strength alloys of the type suitable for glass-to-metal or

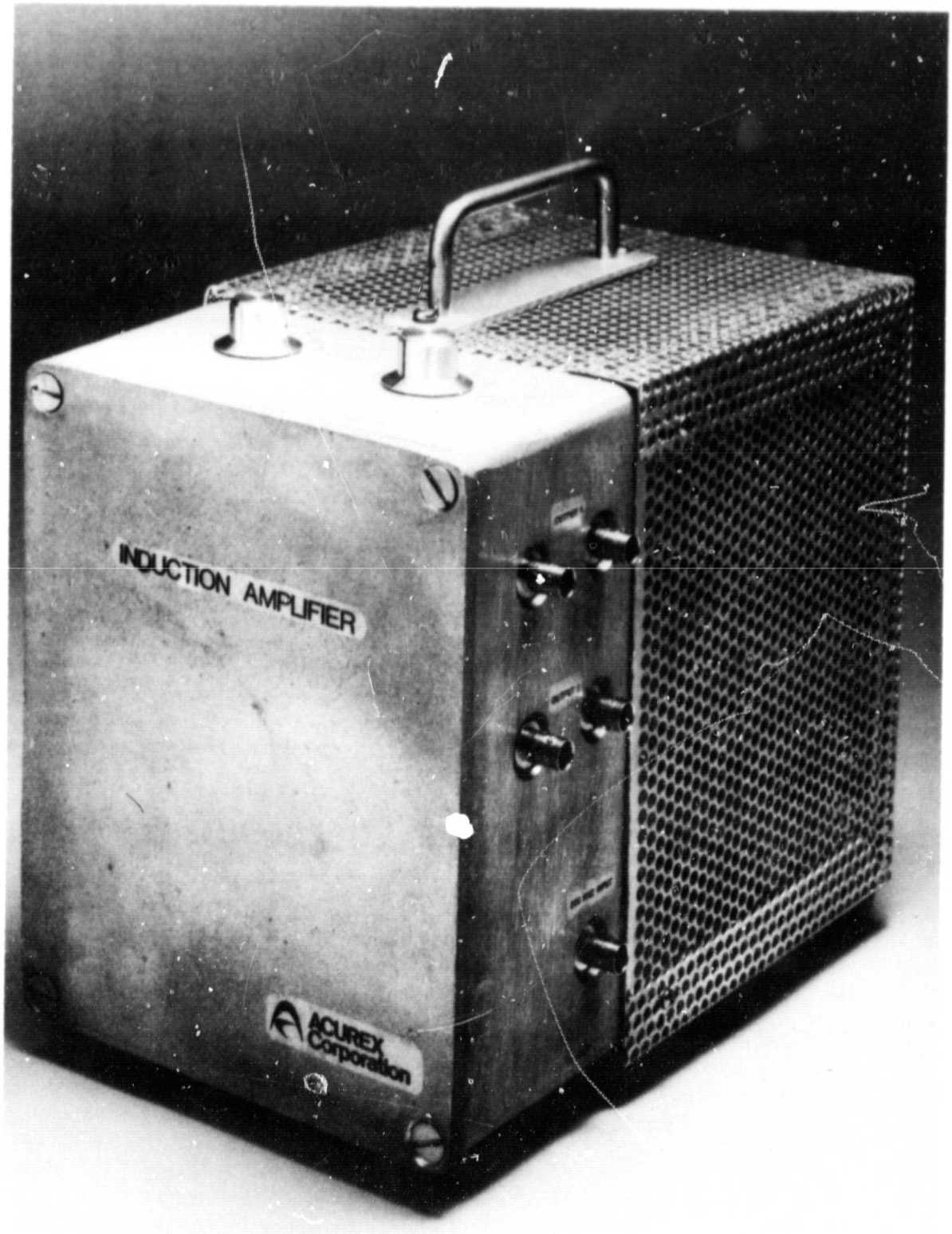

Figure 2-6. Induction Amplifier

glass-to-ceramic seals. These alloys, such as kovar or dumet, are required due to their low thermal expansion coefficients. The design goals of this program called for higher centrifugal loading and higher ambient temperatures than were practical with these metals.

The Phase I Report (reference 1) discusses package development efforts based on high-strength (heat-treatable) alloys and epoxy feed-through seals. Although seals were developed which passed high temperature centrifuge tests and soldering tests, the report expressed some reservations about the long-term durability of these seals.

An added problem with the packages was that potential users of the system were concerned about the weight of the transmitter modules, which was about 30 grams each. They were concerned that this weight would become excessive in a large system, containing 50 or more modules at high centrifugal loading. Several industry users requested that Acurex explore the alternative of fabricating the packages from titanium, rather than the heat-treated 17-4 ph stainless steel which had been planned. This was done. The studies indicated that titanium was structurally suitable and would permit a 40 percent reduction in module weight but with a 15 percent increase in cost.

In recent years several manufacturers of hybrid microcircuits have begun to manufacture circuits on glass-reinforced thermosetting plastic substrates, rather than ceramic. Their primary incentive for this material substitution was economic.

Acurex decided to investigate these substrates because it was believed that their greater flexibility would permit them to be enclosed in less rigid (and thus lighter-weight) metal packages than were necessary for the brittle ceramic substrates.

A quantity of sample substrates was obtained. These substrates were made from copper-clad glass-reinforced polyimide. The copper was plated with gold (over a nickel diffusion barrier).

The substrates were subjected to a variety of tests to determine their suitability for use in high-temperature, high G, hybrid circuits. These tests included:

- Wire bonding tests
- Die-attached tests
- Thermal cycling
- Extended high temperature exposure and thermal creep

The wire bonding tests included evaluation of bonds for mechanical strength and electrical conductivity after the extended high temperature exposure. The substrates passed all of these tests with flying colors.

Another Acurex program provided the first opportunity for the application of this new substrate material. In this application there was a need for a longer than normal substrate. It was advantageous to use the glass-polyimide substrate to reduce the possibility of the cracking under high G's.

Substrates procurred for this program failed wire bonding tests. Specifically, the ultrasonic aluminum wire bonds showed poor mechanical strength after high temperature aging. Examination of the failed bonds revealed that the bonding wire was still attached to the gold plating, but the gold had separated from the nickel diffusion barrier which was plated beneath it. This problem only occurred after high temperature aging.

Subsequent investigations eventually indicated that the problem was due to organic contaminants in the nickel plating. Several sample batches with good control of nickel purity were obtained which did not exhibit the problem.

It was also discovered that the problem was less likely to occur if the bonding pressure was reduced -- even though this required an accompanying increase in ultrasonic power level and duration.

As stated previously, it was intended to use the glass-polyimide substrates inside a metal package which could be more flexible, and thus lighter than the package needed for the ceramic substrate. This in itself offered advantages.

The most significant packaging advance consisted of the complete elimination of the metal enclosure. Figure 2-7 illustrates that packaging method. The package consists of only a substrate and a lid. Note that the edges of the substrate have been extended to provide external terminations for the connections to the strain gages, induced power, the antenna plate, and for programming the carrier frequency of the frequency synthesized transmitter. This eliminates the need for feed-through terminals.

The lid of the package is compression molded from carbon reinforced polyimide resin. This material offers a significantly higher strength-to-weight and stiffness-to-weight ratio than any metal. It also promises lower ultimate manufacturing costs. Polyimide resin was chosen instead of epoxy because of its higher temperature capability. The cured composite shows no degradation in flexural modulus at temperatures up to 600 degrees farenheit.

Figure 2-4 shows the method of stacking multiplex transmitters in a single cavity of a turbine rotor. Note that the transmitter lid serves as a support base for the substrate of the transmitter which is radially inside of it.

Appendix A is a stress analysis of the package.

Each transmitter weighs 4.5 grams. A stack of four transmitters weighs only 18 grams, which is about half the weight of a single transmitter constructed by the earlier packaging method.

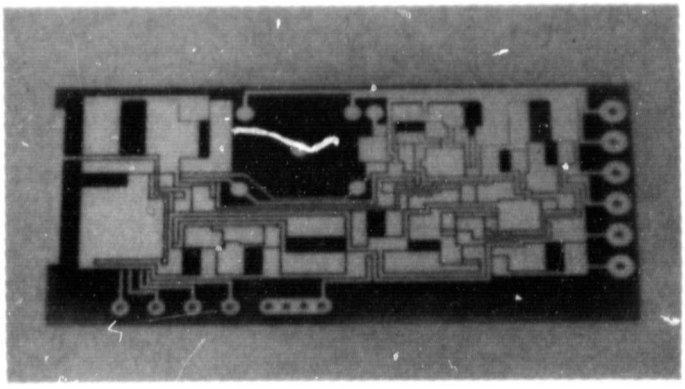

A. Bare glass-polymide substrate

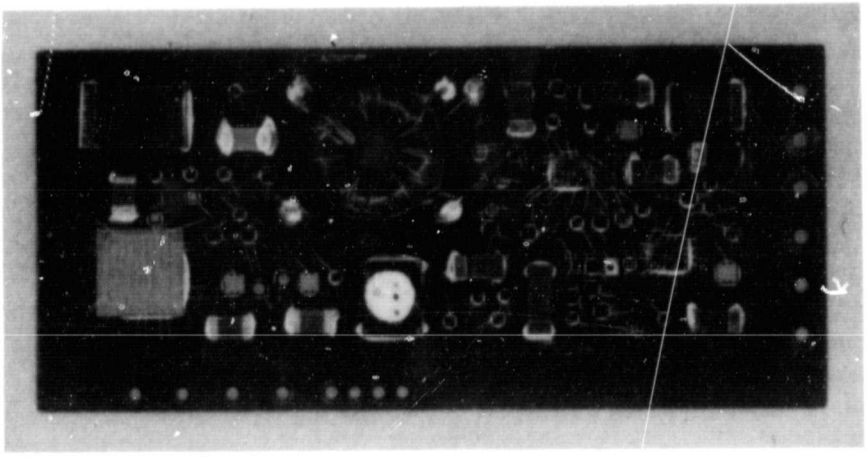

B. Substrate with hybrid components attached and wire-bonded

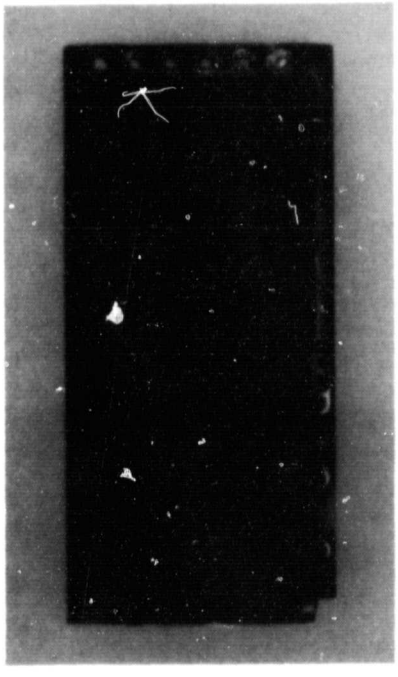

C. Finished transmitter (carbon-polyimide cover over hybrid components)

Figure 2-7. Dynamic Strain Transmitter Packaging

2.5 DESIGN GOALS

The original objective, as specified by NASA, are outlined in Table 2-1. Note that both minimum requirements and design objectives are stated. These requirements and objectives, were derived from a study of industry requirements conducted under sponsorship of the Air Force Propulsion Laboratory (reference 2).

SECTION 3

STATIONARY ELECTRONICS

Stationary electronics consists of the following functional blocks. Each block is discussed in the paragraphs that follow.

- Mainframe
- RF Coupling Link Stator Assembly
- Dynamic Strain Receiver
- Induction Power Supply and Stator Unit

These units are designed to operate under ambient room conditions of +15 to +55°C.

3.1 DYNAMIC STRAIN RECEIVER

The Dynamic Strain Receiver is a double-conversion, superheterodyne, frequency synthesized receiver (refer to figure 3-1). Channel selection of the receiver is accurately locked to the transmitter, since the 200 kHz frequency of the induction power supply is used for the phase lock loop in both the receiver and transmitter.

Circuit design consists of an RF AGC input amplifier (N.F. 4-5 dB), followed by a mixer and two intermediate frequency amplifiers. The IF amplifiers operate at 10.7 MHz and have wide bandwidth bandpass filters. the IFs drive a second mixer and third IF stage where the frequency is lowered to approximately 594 kHz. This lower frequency is required for driving the digital FM discriminator. Provision is included in the receiver for detecting

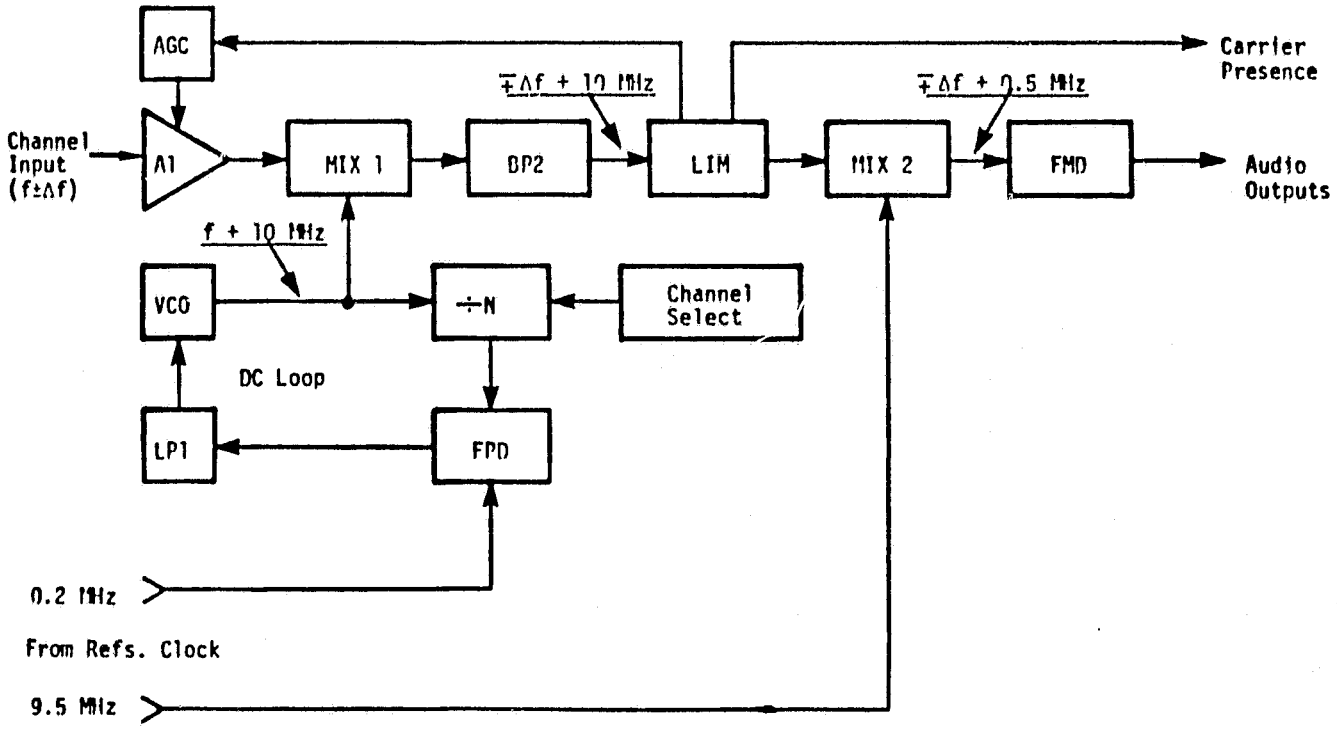

Legend

A1 = Variable gain RF amplifier
AGC = Automatic gain control circuit
BP2 = Bandpass filter (10 ± 0.1 MHz)
MIX 1 = Double-balanced mixer
LIM = Voltage limiter
MIX 2 = Digital frequency mixer
VCO = Voltage-controlled oscillator (20.4 - 30.6 MHz)
LP1 = Lowpass filter
FPD = Digital frequency and phase detector
÷N = Divide-by-N counter
FMD = FM detector
f = Channel center frequency (10.4 - 20.6 MHz)
Δf = Frequency deviation (75 kHz)

Figure 3-1. Superheterodyne Receiver

and indicating the 50 kHz gauge continuity test signal and channel acquisition. It should be noted that the input to the first mixer stage is a combination of signals from the frequency synthesizer and input signal. The stage is followed by the first and second IF stages, then a second mixer and third IF. The second mixer has an injection frequency originating from the local oscillator which is housed in the mainframe. The local oscillator drives all operating receiver modules in parallel. One active limiter stage precedes the digital FM discrimator.

3.2 MAINFRAME

The mainframe is of card cage design. It houses the local oscillator and power supply and twelve Dynamic Strain Receiver channels. The local oscillator has a divider which determines the induction power supply frequency. A wide-bandwidth bandpass filter is at the RF amplifier input circuit and restricts the total RF signal to the desired spectrum. The filter decreases interference from other RF sources and transmitter harmonics.

3.3 200 kHz POWER OSCILLATOR

This device provides the primary power for the induced power system. The most important design consideration was that the circuit must have exceptionally low harmonic content. This is essential because the transmitter carrier frequencies are all phase-locked multiples of the 200 kHz power induction frequency. Any harmonics above the fiftieth harmonic would be at the same frequencies as the transmitter carriers.

Low harmonic content was achieved with an L-C oscillator which has its amplitude controlled by an AGC loop. This oscillator is followed by a low distortion power amplifier. The harmonic content is further controlled by resonating the inductance of the primary induction coil (in the turbine) with a capacitor in the output of the power amplifier. A current sensing circuit

is also provided to protect the system in the event of an accidental short circuit of the induction coil, or its wiring.

3.4 DESIGN GOALS

Some design goals for the stationary electronics are implied to a large part by the General System Performance Goals. Specific receiver specifications are defined in table 3-1.

Table 3-1. Receiver Input and Output Specifications

Receiver Input Specifications		
R.F. Signal Input	Number of channels Adjacent channel spacing Carrier frequency range Single carrier rms level Combined carrier peak level Type of modulation Frequency deviation Modulation frequency range	58 0.2 MHz 11.5 MHz to 22.8 MHz 0.1 mV to 10 mV 400 mV maximum FM ±75 kHz nominal 20 Hz to 50 kHz
Digital Inputs	Number of channel select line Type of code	2 x 4 2 -- digit complement of 9's complement

Receiver Output Specifications		
Analog Outputs	Signal to noise ratio (20 Hz to 50 kHz) Harmonic distortion Voltage level stability Output peak voltage	>40 dB <1 percent ±1 percent ±2 V
Composite Output	Frequency range	20 Hz -- 40 kHz (-3 dB)
Monitor Output	Frequency range	20 Hz -- 20 kHz (-3 dB)
Digital Outputs	Carrier strength indicator: yields an "INVALID DATA" output when the desired rms carrier level drops below 0.1 mV	
	Gage failure indicator: yields an "INVALID DATA" output for open gages Detection of the 50 kHz self-test signal is used for this purpose	

SECTION 4

TEST CRITERIA AND RESULTS

The main objective of the tests presented in this section were to demonstrate performance of the multi-channel wireless data coupling system as set forth under NASA Contract NAS3-20796. Specific objectives were to characterize under hostile environment conditions, four hybrid Dynamic Strain Transmitters and one Induction Coupler (for power requirements). The system is intended to reach temperatures of up to 175°C at rotational static g-forces of up to 50,000 g's.

Additional tasks were to characterize those portions of the system operating under normal environmental conditions such as the Induction Coupled Power Driver, two frequency synthesized receivers with signal conditioning, and one main frame assembly for interfacing and powering the receivers.

4.1 OPERATIONAL TESTING OF RECEIVER MODULES (+15 to +40°C)

4.1.1 Phase Shift Accuracy

This accuracy shall be measured signal-to-channel output and channel-to-channel output. For this test, the rotor is stationary with an air gap between rotor and stator of first, 0.035 inch and then, 0.070 inch A dynamic strain channel is simulated by a precision FM Signal Generator, modulated from 10 Hz to 30 kHz. The generator drives a transmitter antenna and provides an input to the receiver over the range of 10 to 500 microvolts. Phase shift is measured from input-to-channel and channel-to-channel.

Tests were conducted per figure 4-1. A Tektronix 475 oscilloscope was synchronized to the input signal, with arbitrary calibration of the horizontal axis for measuring phase shift. This was an end-to-end test whereby any delays due to filter stages in the receiver were measured and accounted for. Frequency response was measured in 10 Hz increments from 10 to 100 Hz, 100 Hz increments from 100 Hz to 1 kHz increments from 1 to 30 kHz. Results of these tests are given in graphs 1 and 2.

The amplitude and phase response is dominated by the characteristics of the receiver low-pass filter, which removes the 596 kHz second IF frequency after FM detection. This filter is manufactured with component value tolerances of ±1 percent. Thus phase characteristics will be quite similar between channels, satisfying the phase correlation requirements given in the performance goals of table 1-1.

4.1.2 Intermodulation Distortion

This test was used to measure the IMD of the transmitter carrier, per standard techniques, using a Spectrum Analyzer. Equipment set-up for this test is as shown in figure 4-2.

Results of this test show that IMD is 50 dB from the transmitter's RF level. Capture ratio is 38 dB at the same frequency.

4.2 OPERATIONAL TESTING OF THE MAIN FRAME (+15 to +40°C)

4.2.1 Power Supply Voltages

These voltages are to be within ±2 percent of the nominal stated levels. The power supply voltage testing over temperature were conducted in the main frame since the transformers, rectifiers and filter capacitors are located there. The receiver main frame was fully loaded with the following components and the receiver +5 volts were connected to the Induction Amplifier.

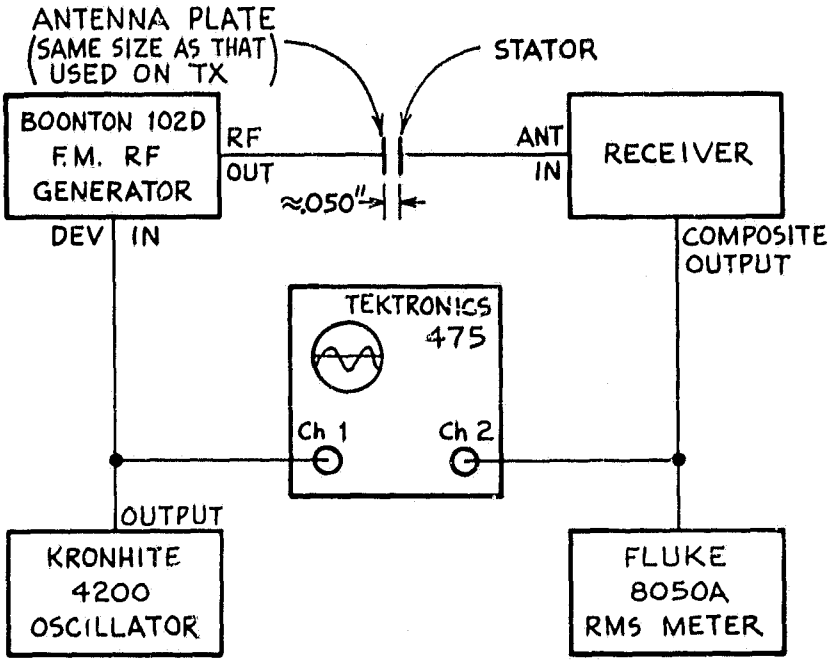

Figure 4-1. Receiver Frequency Response Test

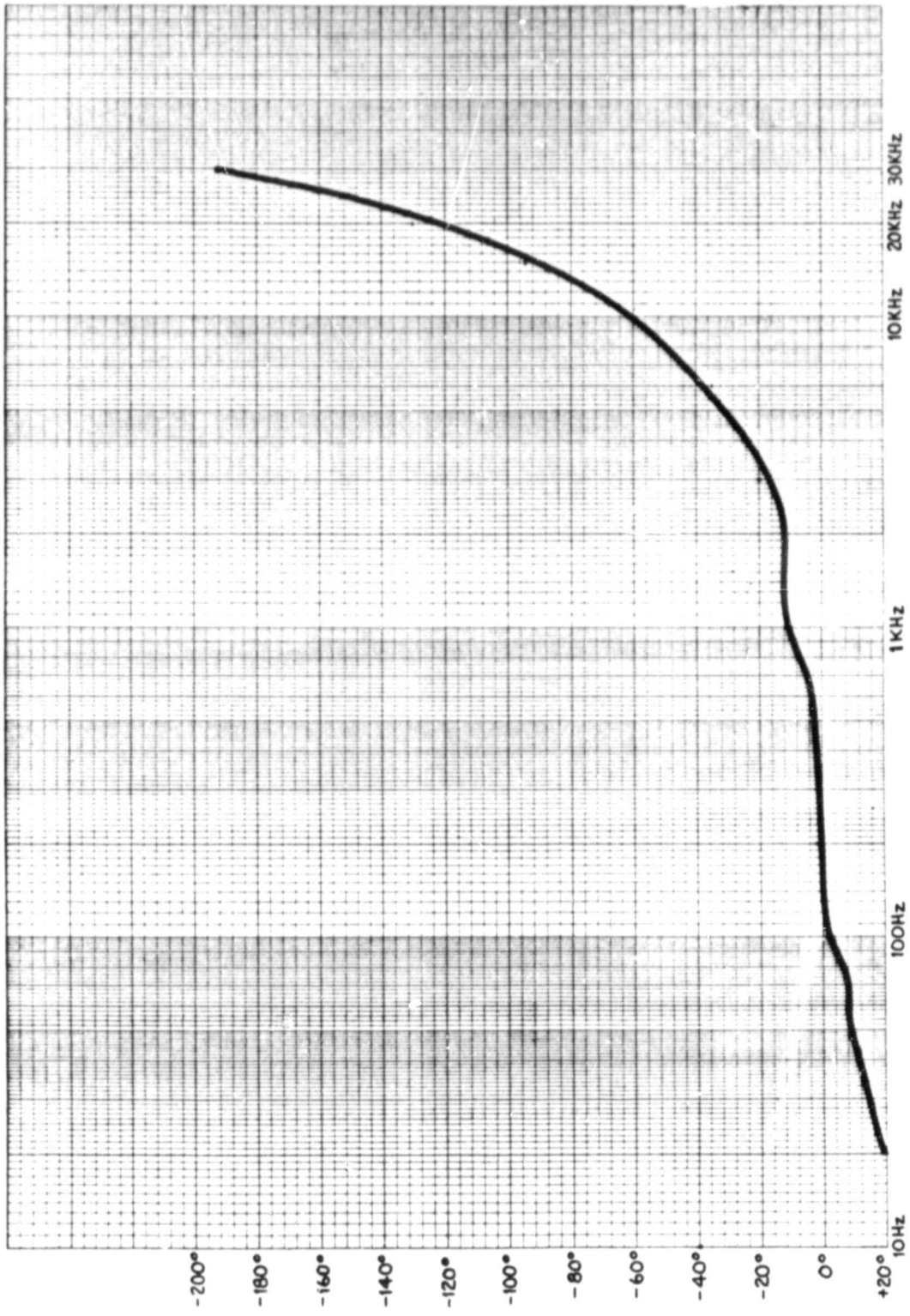

Graph 1. Phase Response of Receiver

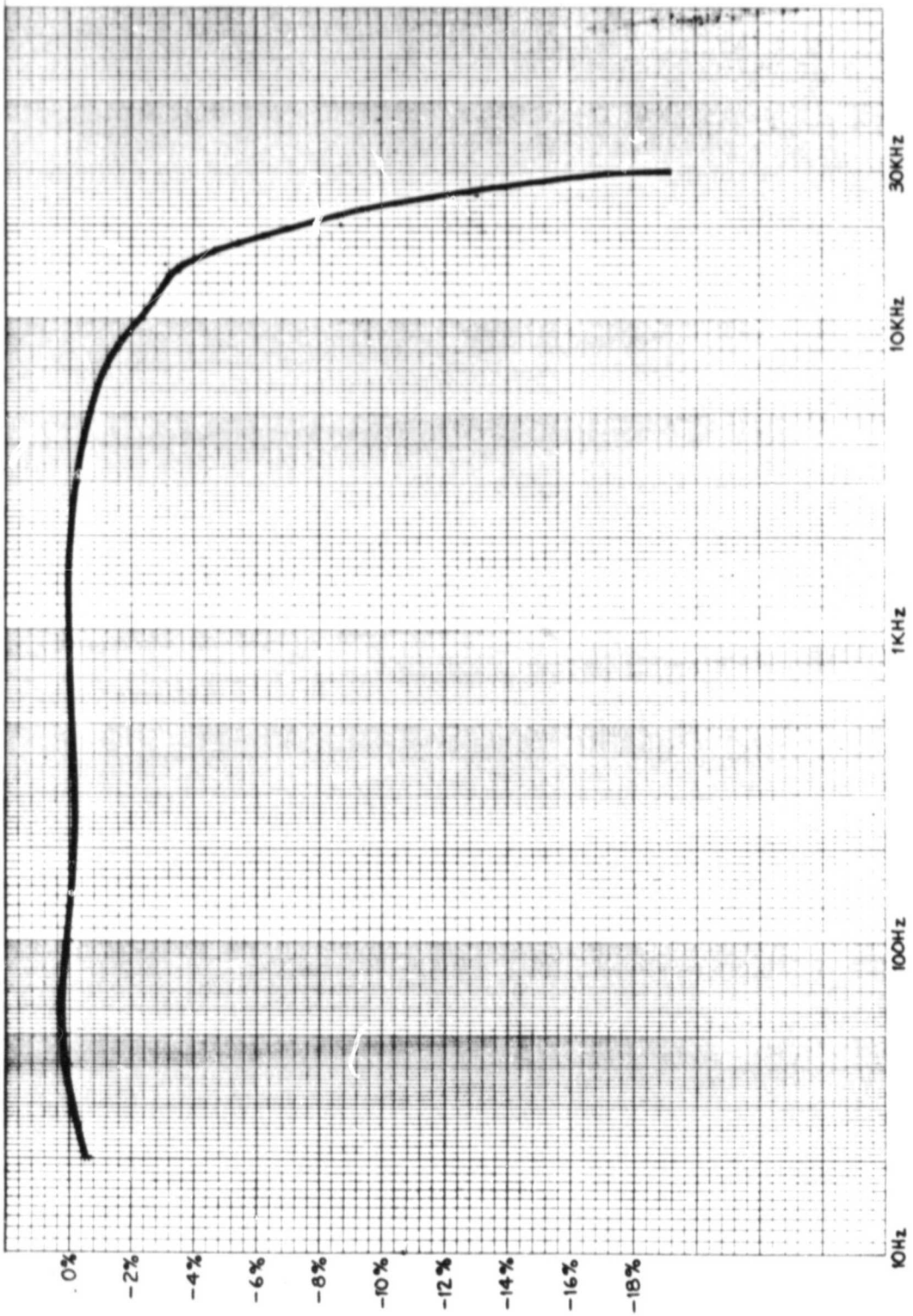

Graph 2. Receiver Amplitude Response vs. Frequency

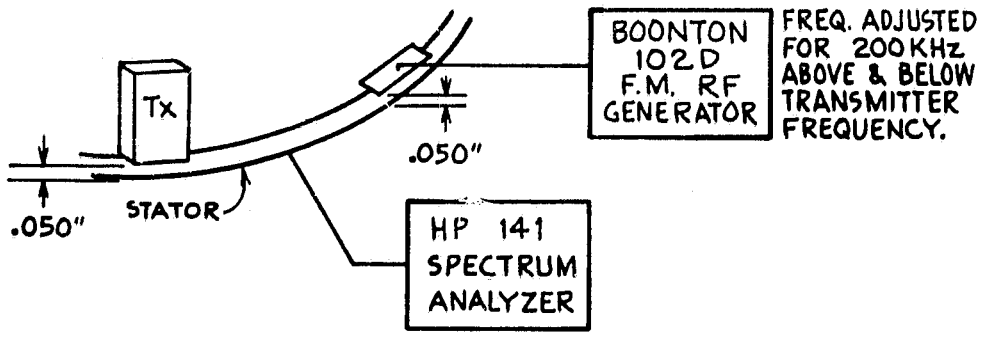

Figure 4-2. Intermodulation Distortion Test Set-up

A. Power Supply Card

B. Dynamic Receiver Cards (3)

C. Static Strain Cards (2)

D. Six-Channel Temperature Cards (2)

The Induction Amplifier was loaded with 5.5 ohms to simulate the stator winding. Test results are shown in table 4-1.

Table 4-1. Power Supply Voltage Test Over Temperature

Voltage	+15°C	Room Temperature	+40°C
+12 V	+11.995	+11.995	+11.998
+12 V ripple	7 mV p-p	4 mV p-p	4 mV p-p
-12 V	-11.990	-12.050	-12.012
-12 V ripple	7 mV p-p	4 mV p-p	4 mV p-p
+5 V	+4.993	+4.998	+4.996
+5 V ripple	7 mV p-p	4 mV p-p	4 mV p-p

4.2.2 Oscillator Frequency Stability

Frequency stability of the oscillator is to be within ±1 percent of the stated frequency over the specified temperature range. The actual ppm temperature coefficient is to be measured.

These tests were conducted at the same time and using the set-up described in paragraph 4.2.1. Results of these tests are contained in table 4-2.

4.3 OPERATIONAL TESTING OF INDUCTIVE POWER SUPPLY (+15 TO +40°C)

4.3.1 Drive Voltage

The induction power supply was tested to ensure the proper drive voltage is placed at the stator and coupled to loaded windings on the rotor. In addition, these tests measure the current consumption of the supply, loaded and unloaded (stator connected and disconnected).

These tests were done concurrently with those in paragraphs 4.2.1 and 4.2.2 and system set-up is as previously described. Results of these tests are located in table 4-3. Current to the induction amplifier was 75 mA at 20 Volts and 80 mA at 30 Volts.

4.4 SYSTEM OPERATIONAL TESTING

4.4.1 Output Signal Linearity

The output signal from the receiver is measured using a quarter, half, and full amplitude, peak-to-peak signal at 1 kHz.

This test was conducted using the test equipment configuration shown in figure 4-3. Results of these tests in V RMS, are shown in table 4-4.

Linear regression of these results shows that all data points are within plus or minus 0.5 percent of a straight line. (Note that the measurement resolution was 0.2 percent).

Table 4-2. Oscillator Frequency Stability

Frequency	+15°C	Room Temperature	+40°C
PLL frequency (Crystal Oscillator)	3169.590 kHz	3169.491 kHz	3169.55 kHz
11.294 MHz	11.29497 MHz	11.29398 MHz	11.29398 MHz

Table 4-3. Operating Testing of Inductive Power Supply

DC Input	+15°C	Room Temperature	+40°C
Rotor Voltages with Simulated Load			
20V	3.173 V rms	2.640 V rms	2.670 V rms
30V	5.174 V rms	4.371 V rms	4.420 V rms
Oscillator Current Consumption			
20V	1.10 Amps DC	0.84 Amps DC	0.90 Amps DC
30V	1.90 Amps DC	1.45 Amps DC	1.55 Amps DC

Table 4-4. Output Signal Linearity

Gauge Input Voltage	Room Temperature		150°C	
	1.6 kHz	16 kHz	1.6 kHz	16 kHz
2.0 V rms	0.623 V rms	0.469 V rms	0.728 V rms	0.509 V rms
1.5 V rms	0.466 V rms	0.348 V rms	0.543 V rms	0.380 V rms
1.0 V rms	0.308 V rms	0.231 V rms	0.358 V rms	0.249 V rms
0.5 V rms	0.156 V rms	0.110 V rms	0.180 V rms	0.121 V rms
0.0 V rms	0.004 V rms		to	0.013 V rms
				.002 V rms

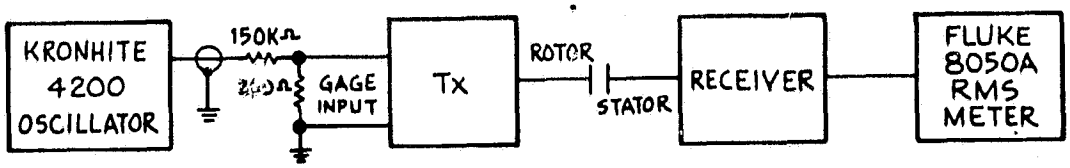

Figure 4-3. Output Signal Linearity, Test Set-up

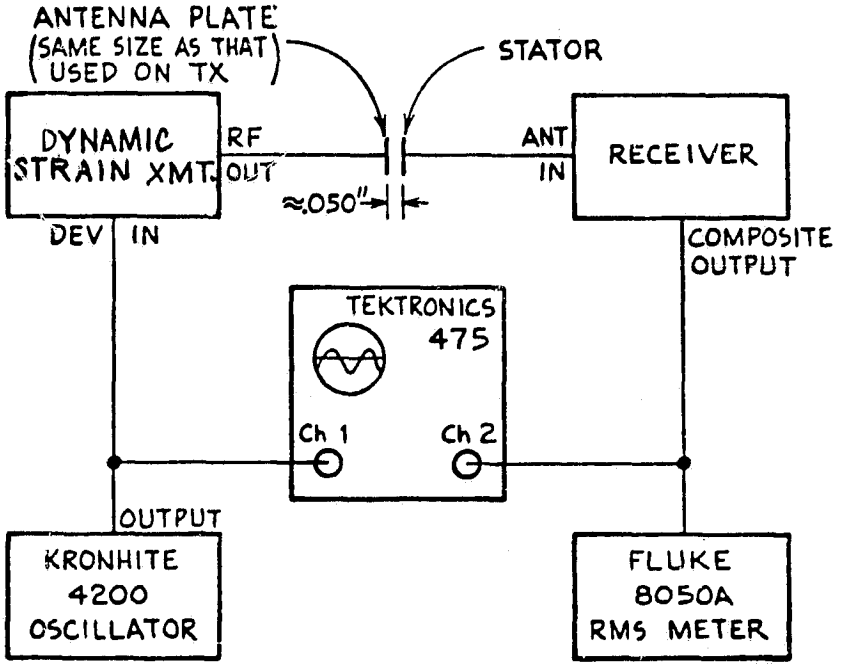

Figure 4-4. Bandwidth and Phase Shift, Test Setup

The data also shows an apparent gain increase of 17 percent due to temperature. However, when used in its intended manner, the transmitter input comes from the strain gage -- not from an external signal generator. The strain gage output is the product of the strain gage resistance variation and the gage excitation current. In temperature compensating each transmitter, the temperature coefficient of this gage excitation current is adjusted to correct for the temperature variations in AC gain apparent in table 4-4. Graphs 3 through 6 show the actual variations in strain sensitivity of four modules when the effects of the compensated excitation current are accounted for.

4.4.2 Measurement of Transmitter Sidebands

In induction powered telemetry systems it is normal for the transmitters to produce sidebands which are spaced away from the fundamental carrier by multiples of the induced power frequency. These sidebands are caused by ripples in the output of the module's internal voltage regulator and by stray coupling within the module. The measured sidebands are shown in table 4-5.

Table 4-5. Transmitter Sidebands

Frequency	Relative Level
Fundamental	0 dB
First sidebands (±200 kHz from fundamental)	-35 dB
Second sidebands (±400 kHz from fundamental)	-56 dB

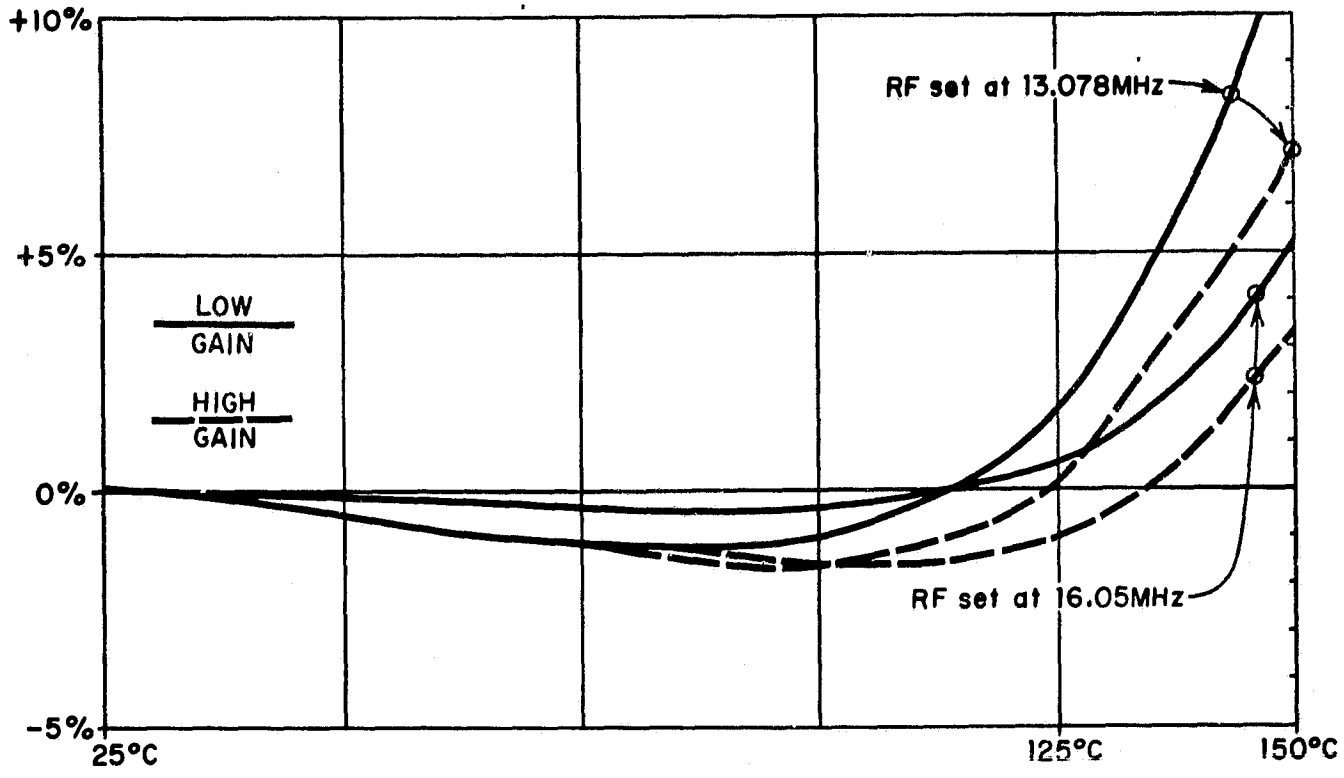

Graph 3. Module No. 2 Gain Vs. Temperature

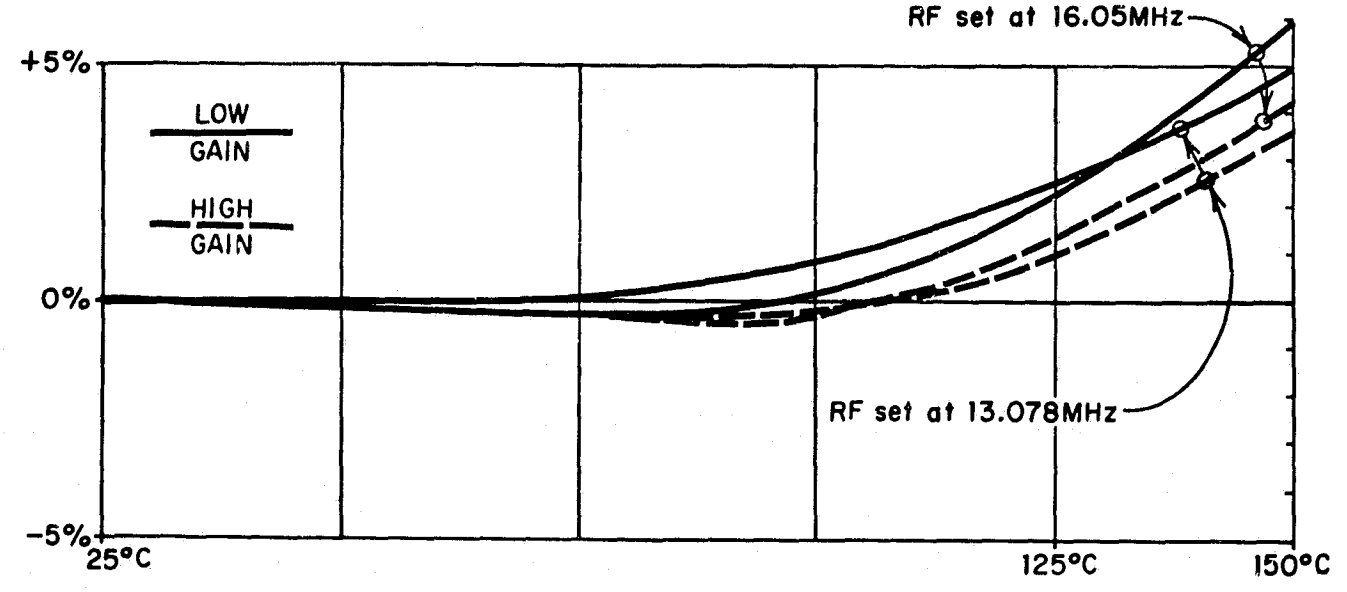

Graph 4. Module No. 3 Gain Vs. Temperature

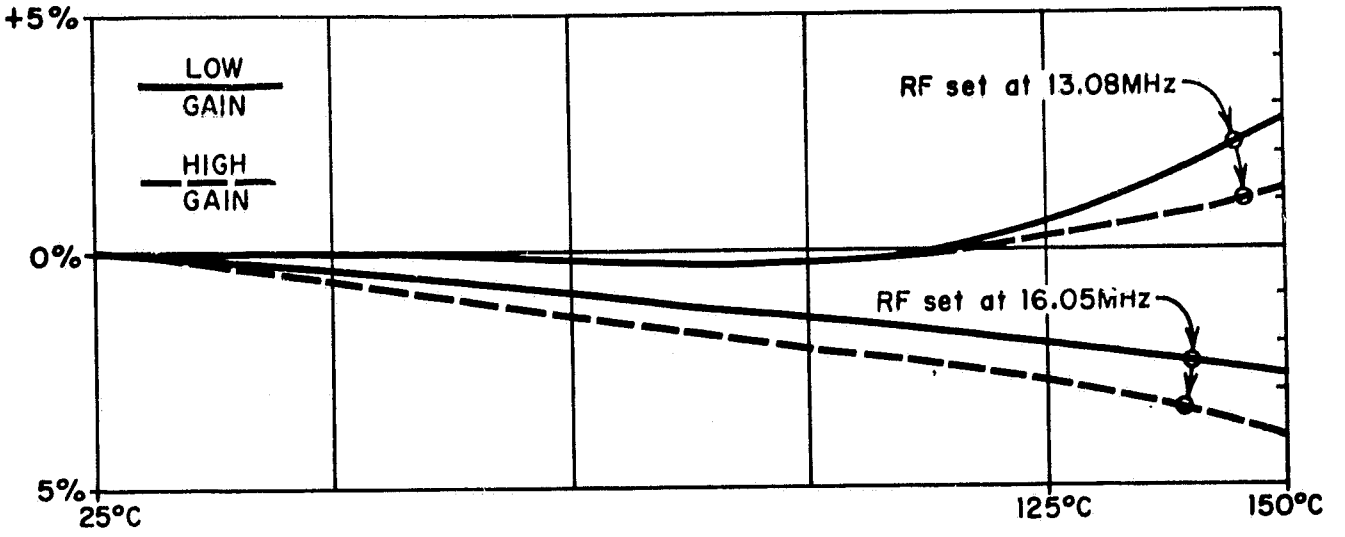

Graph 5. Module No. 7 Gain Vs. Temperature

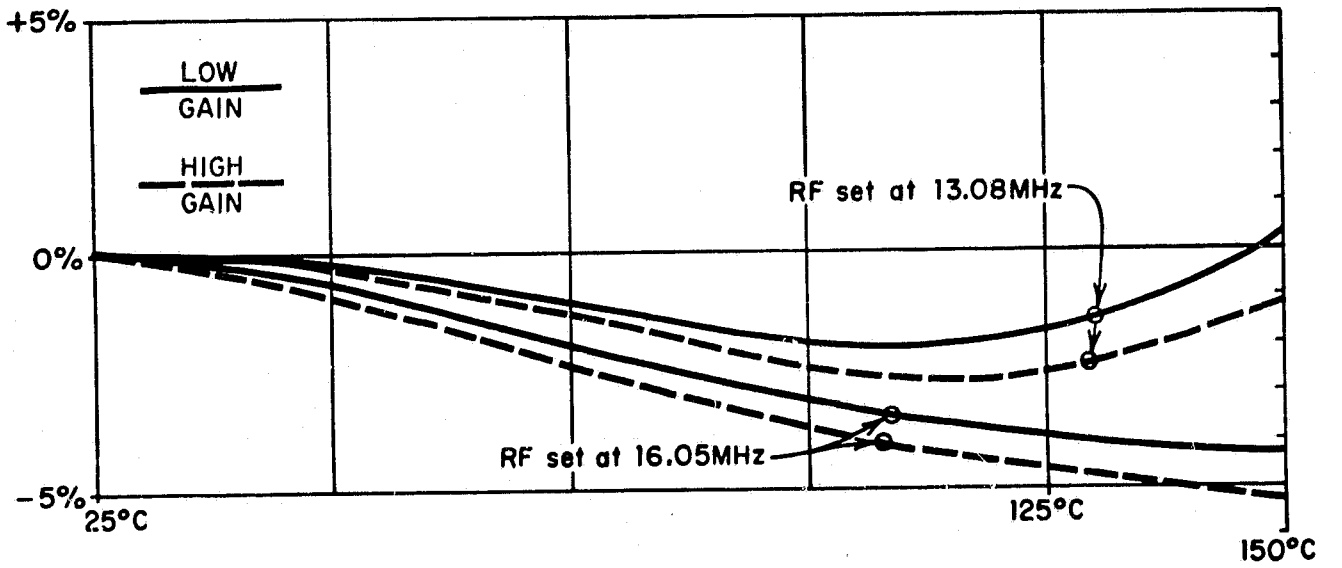

Graph 6. Module No. 8 Gain Vs. Temperature

In this sytem, the sidebands from a transmitter are at the same frequency as the main carriers of other transmitters. The following discussion analyzes the effects which sidebands can have on other transmitters.

4.4.2.1 Effect of Adjacent Channels in the Same Track

Adjacent channels in the same track are spaced 400 kHz apart. Thus, only the -56 dB (second) sidebands are of interest. In the worst case a receiver will be tuned to a carrier plus the second sidebands of the two adjacent channels, which are above and below the carrier. The average sum of the two -56 dB sidebands is a -53 dB interfering signal. The instantaneous peak sum of the two signals could reach -50 dB.

The Phase I report (reference 1, section 3.2.2.4) shows that, in the worst case, the ratio of desired over undesired receiver output data will be approximately the same as the ratio of desired over undesired input carriers. Thus, the average crosstalk produced by the sum of the second sidebands of the two adjacent channels will be -53 dB, which is 0.22 percent. The instantaneous peak crosstalk could reach -50 dB, which is 0.32 percent.

4.4.2.2 Effect of Adjacent Channels in Adjacent Tracks

Adjacent tracks contain transmitters with carriers spaced only 200 kHz away from a given carrier in another track. Thus, the -35 dB (first) sidebands are of interest. Once again, two of these sidebands (from the adjacent transmitters in both of the adjacent tracks) can sum together to interfere with the original carrier. The average sum of these two -35 dB sidebands is -32 dB and the instantaneous peak sum is -29 dB. The track to track coupling was measured in the Phase I report (reference 1, appendix I) as -21 dB, worst case -- for the preferred antenna design. Thus, the -32 dB

average interference becomes -53 dB and the -29 dB instantaneous peak becomes -50 dB. These figures are coincidentially the same as in the case analyzed previously.

4.4.2.3 The Sum of the Previous Two Interferences

A channel can be influenced by both of the aforementioned types of interference simultaneously. In this case the average interference could reach -50 dB (0.32 percent), with an extremely rare instantaneous peak reaching -47 dB (0.45 percent).

4.4.3 Bandwidth and Phase Shift

The bandwidth and phase shift were measured as indicated by figure 4-4. Tests were performed by injecting a simulated strain gage signal into the transmitter (on low-gain) and measuring the output of the receiver. Results of this test are contained in graphs 7 and 8.

4.4.4 System Gain

This was measured by applying an input signal across a 300 ohm, non-inductive resistor, to the input of the transmitter. Circuit is adjusted for full amplitude at the receiver output. Gain is referred to the input.

To conduct this test, the configuration shown in figure 4-3 was used. Results of these tests are shown in table 4-6.

4.4.5 Signal to Noise Ratio

The signal-to-noise ratio was tested using the test set-up shown in figure 4-3. Results of these tests are shown in table 4-7.

4.4.6 Power Variation

These tests were conducted to measure the effects produced on the transmitter, when the Induction Power Supply was varied. As shown on table 4-8, a 24 percent increase in input voltage results in a 1 percent change in output signal.

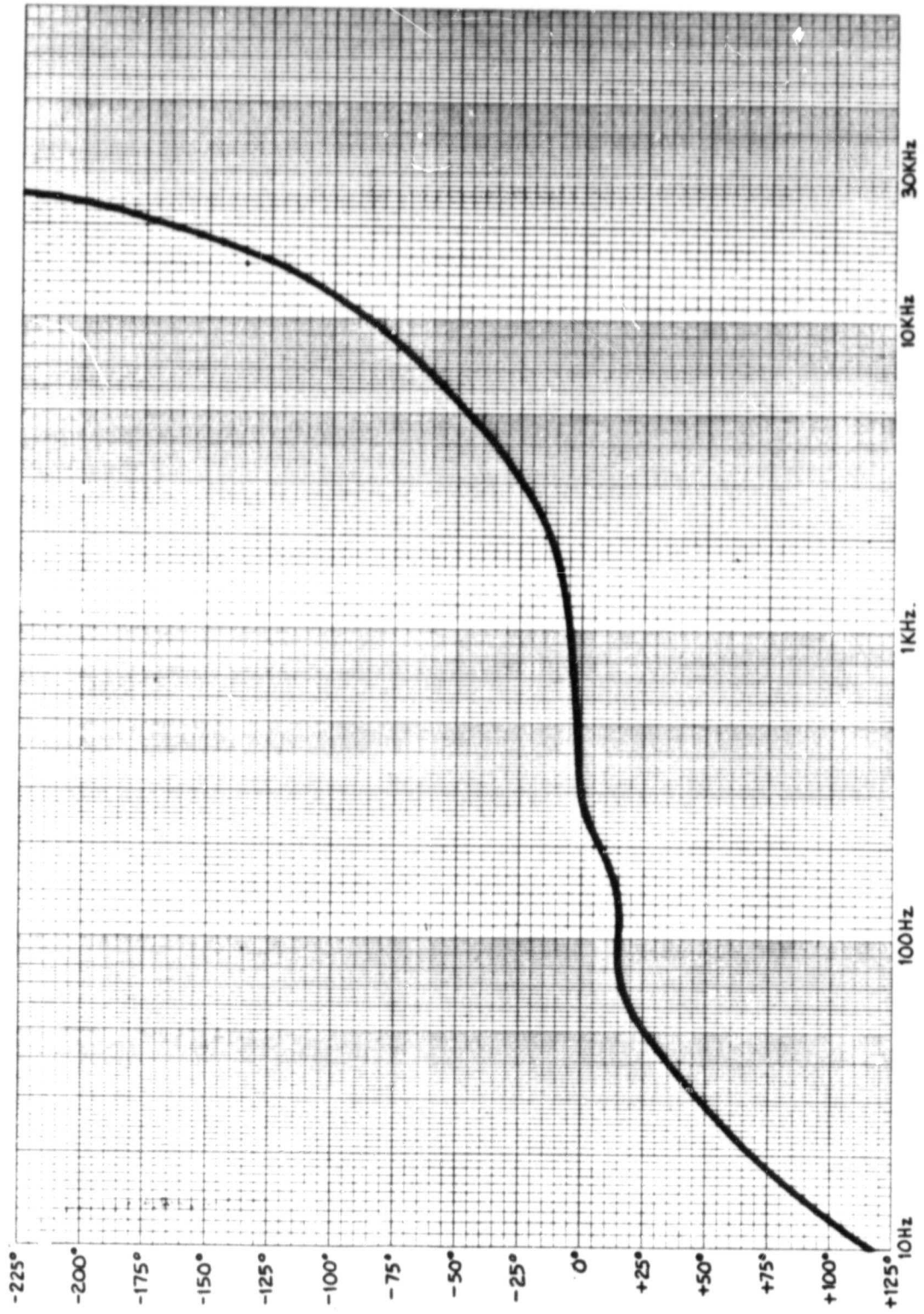

Graph 7. Phase Response of System

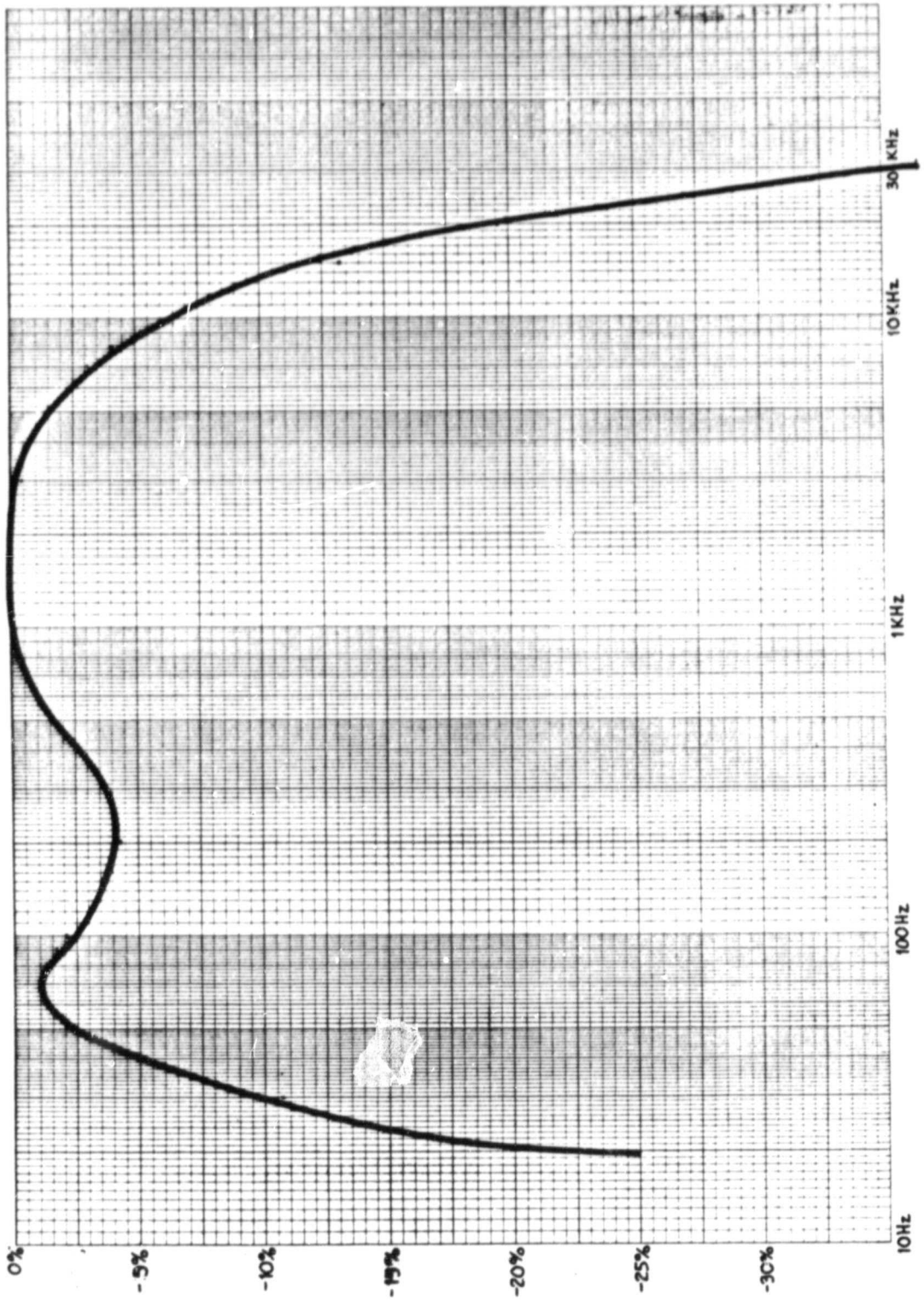

Graph 8. System Amplitude Response vs. Frequency

Table 4-6. System Gain at 1 kHz

Strain Signal 50 Xmtr	Receiver Demonstrated V out	Gain
3.17 mV rms	0.75 V rms	237 (47 dB)

Table 4-7. Signal-to-Noise Ratio

V out (full scale strain)	V out (noise)	Signal to Noise Ratio
0.629 V rms	5.9 mV rms	40.6 dB

Table 4-8. Power Variations

Input Power Voltage	Output Signal Voltage
8.2 V p-p	0.726 V rms
10.2 V p-p	0.733 V rms

4.4.7 Gain Stability vs. Temperature

These tests were conducted at two different temperatures. Initially, the transmitters were heated to 125°C and this temperature was maintained for one hour. The temperature was then raised to 150°C and maintained for one hour. Nominal output signal used in these tests was 1 V peak-to-peak at 1 kHz. The results of the tests, shown in graphs 3 through 6, are derived by the sum of the percent change in gain, plus the percent change of excitation current to the gage.

The variations in gain is most pronounced at the upper end of the temperature range. The gain variations are primarily caused by variations in the sensitivity (dC/dV) of the varactor diodes used to modulate the transmitter voltage controlled oscillator (VCO). The different curves for different carrier frequency settings show how the varactor diode temperature coefficient is dependent on its bias voltage, which is in turn dependent on the setting of the carrier frequency. The system employs the same varactor diodes to both control the carrier frequency (with the phase-locked loop) and to modulate it.

After examination of the results it would appear that an improvement in temperature stability of gain (modulation) can be achieved by employing a separate varactor diode, which is always biased at the same voltage, to perform the modulation. This would permit operating the varactor at its optimum voltage for gain stability, regardless of the carrier frequency selected.

4.4.8 High Temperature Tests

When attempting to operate the transmitters at 175° it was discovered that the SOS power gate, which acts as a buffer between the VCO and the external antenna plate, had insufficient slew rate above 165°C. This is in

contrast to successful tests which were conducted on sample devices submitted by RCA prior to their selection as vendor for the frequency synthesizer chip. It is assumed that process changes were made in the intervening 4-year period which resulted in this problem. If the synthesizers supplied by future vendors exhibit this same characteristic, it will be a simple matter to substitute a discrete RF buffer stage capable of satisfactory operation at 175°.

4.4.9 150° Tests

Due to the problems encountered at 175°C, the transmitters were to be tested at 150°C with a time duration of 24 continuous hours. Results of these tests are shown in table 4-9.

The cause of the failure was determined to be a tantalum capacitor which had become conductive. Tantalum capacitors are the least reliable components used in high temperature circuits but they have demonstrated 150°C lifetimes of hundreds of hours when the applied voltage is derated well below the maximum ratings. The derating criteria used for this design was 25 percent of rating -- which is adequate for operation up to 200°C. The reliability of these components can be increased by screening them with a high temperature burn-in test, if needed.

4.5 SPIN TESTS

4.5.1 40,000 g, 125°C Test

One transmitter was tested at 40,000 g at 125°C for a period of two hours. During this test carrier lock and gage continuity worked well. An increase in noise was noticed and is thought to be due to the selectivity and sensitivity of the receiver. The receiver emits some harmonics onto the RF input line which will affect these parameters.

Table 4-9. Test Results

Time	Date	Temperature	Receiver Output
2:14 p.m.	06/16	Room	1.27 V p-p
3:00 p.m.	06/16	149.8	1.60 V p-p
11:00 p.m.	06/16	149.2	1.60 V p-p
7:00 a.m.	06/17	149.2	50 mV p-p (no modulation)

4.5.2 40,000 g, 150°C Test

A single transmitter was tested at 40,000 g and 150°C. Test results were similar to those achieved in paragraph 4.5.1.

4.5.3 Four Transmitters, 40,000 g, 125°C Test

A stack of four transmitters were installed in a single rotor assembly. When test was initiated at 125°C, only three transmitters would achieve carrier lock. At test conclusion only one transmitter was still functioning properly. After opening the centrifuge and examining the power connections (all good), two of the non-functioning transmitters were working. The third non-functioning transmitter was noted to be off frequency lock (an occurrence which comes from mistriggering of the PLL by insufficient power or too much power).

It is felt that the failure mode for these transmitters was added heat from the centrifuge heating element boosting the temperature over 150°C. The transmitter that was still functioning at the end of the spin test is the only transmitter of this group that functioned at temperatures above 150°C.

4.5.4 Four Transmitters, 40,000 g, 175°C

These tests were not performed due to the failures noted in paragraph 4.4.8.

4.5.5 Four Transmitters, 50,000 g, 150°C

Since all transmitters did not function properly at lower g forces, it was decided to conduct this test using only a single transmitter. The test was initiated and shortly after reaching 50,000 g's the antenna plate on the transmitter disconnected. At this point the test was terminated. It should be noted that the transmitter was still operational on the lab bench when closer coupling of the antenna allowed the transmitted signal to be received by the receiver.

4.5.6 Four Transmitters, 50,000 g, 175°C

These tests were not conducted due to the high failure rate noted in paragraph 4.4.8.

SECTION 5

CONCLUSIONS

A summary of important accomplishments during this phase of the development program is listed below:

- Detailed design of stationary electronics
  - -- phase locked receiver
  - -- receiver signal conditioning cards
  - -- system clock
  - -- induction power supply
- Design of transmitter modules
  - -- development of custom frequency synthesizer IC
  - -- detailed circuit design of dynamic strain transmitter
  - -- breadboard development of static strain transmitter
  - -- development of an entirely new lightweight package
- Fabrication and environmental testing
  - -- stationary electronics
  - -- transmitter module

Although delays in delivery of the frequency synthesizer IC necessitated a reduction in scope (the suspension of development on the static strain and thermocouple transmitters, and an abbreviated development and testing program on the dynamic strain transmitter), the program achieved its

goals of significantly advancing the state of the art of rotating instrumentation. The most noteworthy advances are:

- The development and demonstration of a phase locked system for the control of transmitter carrier frequency
- The development of a new lightweight hybrid electronic packaging system which also promises to reduce future manufacturing costs

5.1 REMAINING TASKS

The next step should be to complete the development of the rotating electronic modules, as originally planned. This would entail additional testing and development of the dynamic strain transmitter (to improve performance and reliability) and completion of development of the static strain and thermocouple transmitters.

Although the transmitter modules fabricated to date have shown poor reliability, there is nothing inherent in the design to suggest that satisfactory reliability will not be ultimately achieved. All of the individual components and processes have demonstrated that capability.

The program has been adversely affected by the 3-year late delivery of the frequency synthesizer integrated circuit. The customer frequency synthesizer employed RCA's standard Universal Array process which uses an existing array of silicon on sapphire CMOS devices and interconnects them with a custom metalization pattern. The logical design of the frequency synthesizer was also standard employing conventional counters, phase comparators, etc.

A few months after delivery of the devices, RCA then announced that they were changing their process and would no longer be willing to supply these devices. Thus an important next step will be to develop an alternative source for the frequency synthesizer IC. Two alternatives are available:

- Adapting one of several new standard frequency synthesizer ICs which have become available in recent years
- Developing a new custom IC, again based on the gate-array process, which is relatively inexpensive.

Some additional development work on the receiver would be appropriate. The sensitivity is below requirements for this application. The inadequate sensitivity appears to be related to insufficient isolation between the low-level input stage and the digital circuitry in the frequency synthesized local oscillator and the FM discriminator. Additional filtering, shielding and isolation are expected to correct this.

5.2 RECOMMENDATIONS

Although original program plans had called for the construction of a large scale (50 to 100 channels) system after the completion of this phase, the tasks discussed above should be completed first. After this is accomplished and satisfactory performance and reliability are demonstrated on a small scale, it will be appropriate to construct the large scale system.

REFERENCES

1. Adler, Alan and Bas Hoeks, "Phase-Locked Telemetry System for Rotary Instrumentation of Turbomachinery -- Phase I," NASA CR-159453, Acurex Corporation, Mountain View, CA, September 1978.

2. Adler, Alan, "Turbine Engine Telemetry Analysis," Acurex Corporation, Mountain View, CA, AFAPL-TR-75-95, November 1975.

3. Adler, Alan, "Multiple Data Channel Wireless Data Coupling System for Transmitting Measured Data From a Plurality of Rotating Sources," U.S. Patent No. 4,011,551. This patent covers the basic method of the phase-locked carriers.

4. Adler, Alan, "Method of Telemetering DC Signals," U.S. Patent No. 3,668,673. This patent covers the method of modulating DC signals as used in static strain or thermocouple telemetry.

5. Adler, Alan, "Multiplexed Telemetering System for DC Signal Source," U.S. Patent No. 3,909,811. This patent covers the method of modulating multiple DC signals and self-calibration, as used in static strain or thermocouple telemetry.

APPENDIX A

STRESS ANALYSIS OF TRANSMITTER CASE

A.1 GENERAL CONDITIONS

Requirements for the design of the transmitter case were survival in an acceleration field of 40,000 g's (40kg's) at a temperature of 175°C. A second design goal was survival in a 50 kg field at 200°C. The following stress analysis was conducted using a 50 kg acceleration field. The case was able to withstand these loads without failure or excessive deflection.

A.1 TRANSMITTER DESCRIPTION

The transmitter case consists of a glass/polyimide composite substrate which also doubles as the bottom of the case, and a compression-molded lid comprising the case top and sidewalls. The molding is formed using oriented graphite fibers and a polymide resin system to provide high strength and extremely light weight. The transmitter case design is shown in figure A-1. The analysis is conducted for the bottom (outboard) transmitter in a stack of 4 transmitters. This transmitter lies on a flat, firm supporting surface, is experiencing the inertial forces resulting from a 50 kg acceleration field, and is carrying the inertial weight of 3 additional transmitters stacked upon it. Each transmitter case supports the weight and limits the deflection of the substrate in the transmitter above it. Since the transmitters stack very precisely, the accumulated weight of all of the transmitters is transmitted

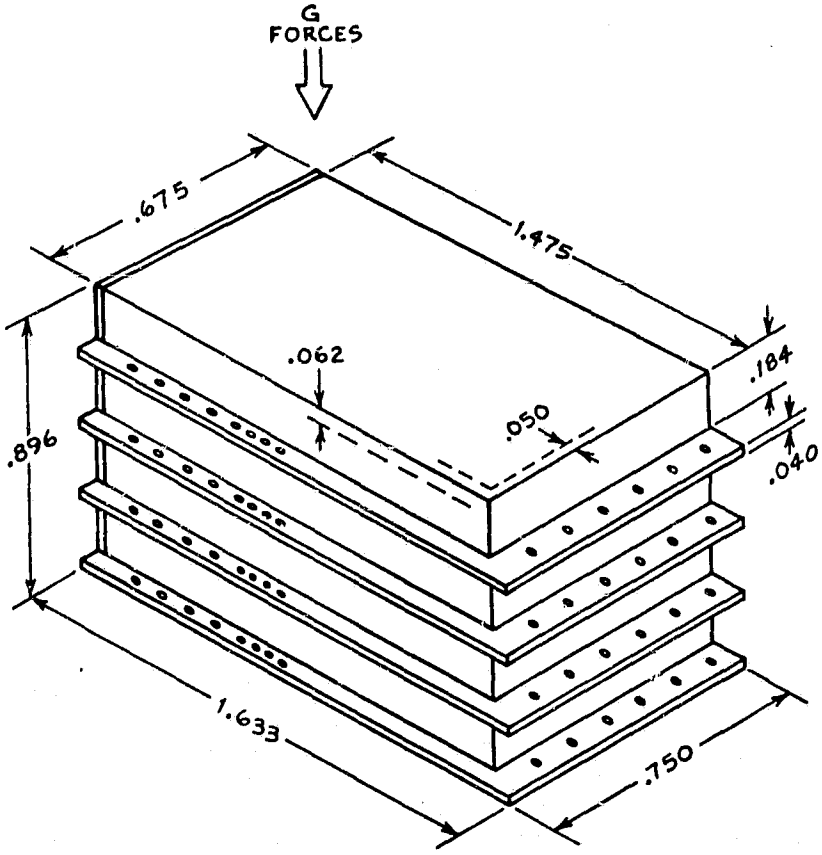

Figure A-1. Stack of Four Transmitters

through the sidewalls of the case to the supporting surface of the rotor, located under the substrate of the bottom (outboard) transmitter.

A.3 STRESSES IN THE TRANSMITTER LID

The geometry of the transmitter lid and substrate are shown in Figure A-1. The top portion of the transmitter lid is a rectangular plate of graphite/polymide, 0.062 in. thick, spanning 1.25 and 0.675 in. over its length and width respectively. The material has a density of 0.057 lb/in.^{3}, producing a uniformly distributed load of 176.7 lb/in.^{2} at 50 kg's. In addition the lid carries the weight of the substrate above, which is 0.032 in. thick glass/polymide. An effective weight, computed for the substrate loaded with electronic components, is 182.9 lb/in.^{2} at 50 kg's. The total effective distributed load on the lid top is 360 lb/in.^{2}.

The maximum bending stress, $\sigma_{B_{max}}$, in the lit top is:

$$\sigma_{B_{max}} = \frac{\beta\, q\, b^2}{t^2} \quad ,$$

where q = distributed load

b = plate width

t = plate thickness

β = coefficient based on length/width ratio

$$\sigma_{B_{max}} = \frac{.6003\ (360)(.675)^2}{(.062)^2} = 25{,}615 \text{ psi}$$

Flexural strength = 48,000 psi @ 600°F, factor of safety, f.s. = 1.87

The maximum lid deflection, y_{max}, is

$$y_{max} = \frac{\alpha\, q\, b^4}{E\, t^3}$$

where E = Modulus of elasticity

α = coefficient based on length/width ratio

$$y_{max} = \frac{.1088\ (360)(.675)^4}{12 \times 10^6\ (.062)^3} = .0028 \text{ in.}$$

Young's modulus is 12×10^6 psi for 30 percent fiber loading in each direction.

A.4 CANTELEVER BENDING IN OVERHUNG SECTION OF SUBSTRATE

Density of substrate $P_s = .0770 \text{ lb/in.}^3 \times 50\ \% = 3{,}850 \text{ lb/in.}^3$

Weight of wire supported by overhung substrate, W_w = 2.50 lb/in. @ 50 kg's per wire

For total distributed load, $w = P_s\ W_s\ t_s + \frac{n\ w_w\ \ell_w}{\ell_s}$

where: w_s = substrate width

t_s = substrate thickness

n = number of wires supported

w_w = weight of a wire/inch of length

ℓ_w = length of wire

ℓ_s = overhung length of substrate

$$w = 3850\ (.775)\ .032 + \frac{5\ (2.50)\ .875}{.100} = 95.48 + 109.38$$

$$w = 204.8 \text{ lb/in.}$$

The bending moment, M_{max}, at the root of the overhung section is;

$$M_{max} = \frac{w\ell^2}{2} = \frac{204.8\ (.100)^2}{2} = 1.024 \text{ lb/in.}$$

The moment of inertia, I, of the section is;

$$I = \frac{wt^3}{12} = \frac{.775\ (.032)^3}{12} = 2.048 \times 10^{-6} \text{ in.}^4$$

The maximum bending stress, $\sigma_{B_{max}}$, is;

$$\sigma_{B_{max}} = \frac{M_{max}C}{I} = \frac{1.024\ (.016)}{2.048 \times 10^{-6}} = 8{,}000 \text{ psi}$$

Where C = Maximum distance to neutral axis

Comparing $\sigma_{B_{max}}$ with the flexural strength of the substrate

$$\text{Safety factor, f.s.} = \frac{48 \text{ KSI}}{8 \text{ KSI}} = 6.0$$

Maximum deflection of the overhung section is;

$$y_{max} = \frac{w\ell^4}{8EI} = \frac{204.8\ (.100)^4}{8\ (2\times10^6)(2.048\times10^{-6})} = .0006 \text{ in.}$$

If wire load is increased to 8 in.;

$$w = 271 \text{ lb/in.},\ \sigma_{B_{max}} = 10{,}486 \text{ psi},\ y_{max} = .0008 \text{ in.}$$

A.4 STRESS CONCENTRATION IN OVERHUNG BOARD SECTION

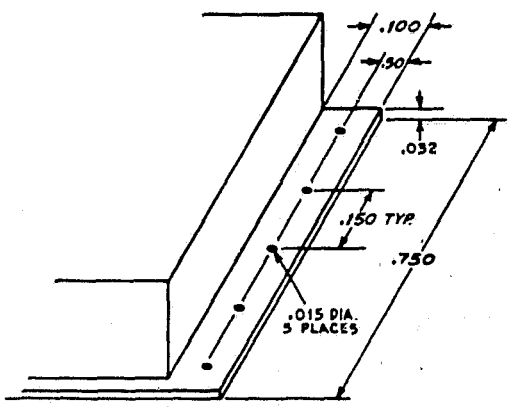

Net width = .750-5 (.015) = .675 in.

Net area = .675 (.032) = .0216 in.^{2}

For bending stress at x = .050 in. with 8 wires;

$$w = 271 \text{ lb/in.} \qquad M = \frac{wx^2}{2} = \frac{271(.05)^2}{2} = .3388 \text{ lb/in.}$$

$$I = \frac{wt^3}{12} = \frac{.675\ (.032)^3}{12} = 1.843 \times 10^{-6} \text{ in.}^4$$

For stress concentration a/b = .015/.150 = .10, K_T = 2.7

$$\sigma_B = K_T \frac{MC}{I} = \frac{2.7\ (.3388)\ .016}{1.843 \times 10^{-6}} = \underline{7,940\ \text{psi}}$$

Where K_T = stress concentration factor

A.6 COMPRESSIVE STRESS IN LID WALL

Weight of lid top @ 50 kg's	=	222.2 lb
Weight of loaded substrate @ 50 kg's	=	240.5 lb
Weight of lid walls @ 50 kg's	=	57.7 lb
Total weight of XMTR	=	520.4 lb
Weight of 4 XMTRS - 1 substrate	=	1,841 lb

Wall area, A_W, = mean perimeter x thickness

$$A_W = 2(.675 + 1.375) \times .050 = .2050\ \text{in.}^2$$

The compressive stress, σ_e, in the bottom transmitter walls is:

$$\sigma_c = \frac{w}{A_W} = \frac{1840}{.205} = 8,980\ \text{psi}$$

adding 178 lb for wire load,

$$\sigma_c = \frac{2019}{.2050} = 9,848\ \text{psi}$$

$$\text{f.s.} = \frac{48}{9.848} = 4.9$$

A.7 LOAD INDUCED CURVATURE IN TRANSMITTER LID

For bidirectional bending;

$$\sigma_x = \frac{ZE}{1-\mu^2} \quad \frac{1}{r_1} + \mu \frac{1}{r_2}$$

where

z = distance from neutral surface

μ = Poisson's ratio

r_1 = radius of curvature in x-direction

r_2 = radius of curvature in y-direction

From

$$\sigma_{max} = 25{,}615 \text{ psi} = \frac{.025\ (12 \times 10^6)}{1 - .45^2} \quad \frac{1}{r_1} + .45\ \frac{1}{r_2}$$

Assume

$$r_2 = r_1\ \frac{a}{b}$$

$$r_2 = 2/196\ r_1$$

where a = lid length

b = lid width

$$25{,}615 = 376{,}176\ \frac{1}{r_1} + \frac{.45}{2.185\ r_1} = 376{,}175\ \frac{1.206}{r_1}$$

$$r_1 = 17.71 \text{ in.}, \quad r_2 = 38.70 \text{ in.}$$

This curvature is induced into the substrate of the transmitter above, and into the silicon chips on the substrate (assuming no flexural stiffness is added by the silicon)

$$\text{Stress in the chip, } \sigma_B = \frac{ZE}{1 - \mu^2} \quad \frac{1}{r_1} + \mu\ \frac{1}{r_2}$$

Chip is .025 in. thick, E = 27 x 10^6 psi, tensile strength = 27 ksi, μ = .28

$$\sigma_B = \frac{.0125\ (27 \times 10^6)}{1 - 28^2} \quad \frac{1}{17.71} + 28\ \frac{1}{38.70} = \underline{23{,}328 \text{ psi}}$$

$$fs = \frac{23.3}{27} = 1.16 \text{ @ } 50 \text{ kg's}$$

A.8 SHEAR STRESS IN EPOXY BOND BETWEEN CHIP AND SUBSTRATE

The major dimension of the largest chip is .185 inches. Assuming that this chip was located at the point of maximum curvature on the substrate, and that the substrate transferred its entire inertial weight to the lid of the transmitter below (substrate chip had no appreciable bending stiffness of its own), the substrate would conform to the contour of the lid. The maximum curvature (minimum radius) appearing on the lid is 17.71 inches (section A-7).

The radius of curvature of the lower surface of the substrate is 17.7100 inches. The radius of the upper surface (interface) is 17.71 - .032 = 17.6780 inches, which is equal to the lower surface (interface) radius of the chip. The radius of the midplanes of the chip and substrate are 17.6655 and 17.6940 inches respectively.

Beginning with a length of .185 inches, the arc length of the interface surface of the unbonded curved chip, $S_{chip} = .185 \left(\frac{r_{interface}}{r_{midplane}}\right)$

$$S_{chip} = .185 \left(\frac{17.6780}{17.6655}\right) = .185131$$

likewise for the curved unbonded substrate,

$$S_{subst} = .185 \left(\frac{17.6780}{17.6940}\right) = .184833$$

The difference in surface length, $S_{chip} - S_{subst}$, is equal to .000298 inches. This must be accommodated by compression of the chip and tensile stretching of the substrate. The necessary force to accomplish this is transmitted through the bond layer as a shear force

So we have $\Delta L_{chip} = \frac{F_{chip}\, L}{A_{chip}\, E_{chip}}$

and

$$\Delta L_{substrate} = \frac{F_{substrate}\, L}{A_{substrate}\, E_{substrate}}$$

$F_{chip} = F_{substrate}$ = shearforce in bond

$\Delta L_{chip} + \Delta L_{subst} = .000298$

For a unit width of chip and substrate,

$$F_{chip} = \frac{\Delta L_{chip}\, A_{chip}\, E_{chip}}{L} = \frac{\Delta L_c\ (.025)\ 15.5 \times 10^6}{.185} = 2.094 \times 10^6\ \Delta L_{chip}$$

$$F_{subst} = \frac{\Delta L_{subs}\, A_{subst}\, E_{subst}}{L} = \frac{\Delta L_s\ (.032)\ 2 \times 10^6}{.185} = 3.459 \times 10^5\ \Delta L_{sub}$$

$\Delta L_{subst} = .000298 - \Delta L_{chip}$

Substituting

$F_{subst} = 3.459 \times 10^5\ (.000298 - \Delta L_c) = 103.092 - 3.459 \times 10^5\ \Delta L_c$

Setting $F_{chip} = F_{subst}$, and solving for ΔL_{chip},

$\Delta L_{chip} = .000042$ inches

$$F_{chip} = \frac{.000042\ (.025)\ 15.5 \times 10^6}{.185} = 88.5 \text{ lb}$$

Therefore shearforce F = 88.5 lb

interface area (unit width) = .185 (1.00) = .185 in^2

shearstress, $\tau = \frac{88.5}{.185} = 478$ psi

Since the allowable stress ≈ 4,000 psi,

the factor of safety = $\frac{4,000}{478} = 8.37$